CIVIL ENGINEERING STUDIES
Illinois Center for Transportation Series No. 08-029
UILU-ENG-2008-2017
ISSN: 0197-9191

CHARACTERIZATION OF LOW TEMPERATURE CREEP PROPERTIES OF CRACK SEALANTS USING BENDING BEAM REHOMETRY

Prepared By

Imad L. Al-Qadi
Shih-Hsien Yang
University of Illinois at Urbana-Champaign

Mostafa A. Elseifi
Louisiana State University

Samer Dessouky
University of Texas at San Antonio

Amara Loulizi
Re'seau National Universitaire, Tunisia

Jean-François Masson
National Research Council of Canada

Kevin K. McGhee
Virginia Transportation Research Council

Research Report ICT-08-029

Illinois Center for Transportation

November 2008

Technical Report Documentation Page

1. Report No.	2. Government Accession No.	3. Recipient's Catalog No.
FHWA-ICT-08-029		

4. Title and Subtitle
CHARACTERIZATION OF LOW TEMPERATURE CREEP PROPERTIES OF CRACK SEALANTS USING BENDING BEAM REHOMETRY

5. Report Date
November 2008

6. Performing Organization Code

7. Author(s)
Imad L. Al-Qadi, Shih-Hsien Yang, Mostafa A. Elseifi, Samer Dessouky, Amara Loulizi, Jean-François Masson, Kevin K. McGhee

8. Performing Organization Report No.
ICT-08-029
UILU-ENG-2008-2017

9. Performing Organization Name and Address

University of Illinois at Urbana Champaign
Department of Civil and Environmental Engineering
205 N. Mathews Ave, MC-250
Urbana, Illinois 61081

10. Work Unit (TRAIS)

11. Contract or Grant No.
VTRC Project # 67775
TPF-5(045)

13. Type of Report and Period Covered
Technical Report

12. Sponsoring Agency Name and Address

Federal Highway Administration
400 North 8th Street, Room 750
Richmond, VA 23219-4825

Virginia DOT – Lead State
1401 E. Broad St
Richmond, VA 23219

14. Sponsoring Agency Code

15. Supplementary Notes

16. Abstract

Crack sealing has been widely used as a routine preventative maintenance practice. Given its proper installation, crack sealants can extend pavement service life by three to five years. However, current specifications for the selection of crack sealants correlate poorly with field performance. The purpose of this research was to develop performance guidelines for the selection of hot-poured bituminous crack sealants at low temperature. In this part of the research, the creep behavior of crack sealant at low temperature is measured and performance criteria for material selection were developed. Because various pavement and State agencies are well acquainted with and own the Bending Beam Rheometer (BBR), which was developed during the Strategic Highway Research Program (SHRP), an attempt was made to utilize the same setup to test hot-poured bituminous-based crack sealants. Testing conducted in this research project indicated that the standard BBR was inappropriate for testing soft bituminous-based hot-poured crack sealant, even at -40°C. The measured deflection exceeded the BBR limit, for some sealants, after only a few seconds of loading. To address this issue, the moment of inertia of the tested beam was increased by doubling its thickness (from 6.35mm to 12.7mm). For the new beam dimensions, it was found that only 4% of the beam center deflection is due to shear, a value deemed acceptable for sealant evaluation and comparison.

In an effort towards developing a robust testing procedure, 15 sealants from various manufacturers were included in the study and tested between –4°C and –40°C. In addition, five sealants, which have known field performance, were tested to validate the laboratory results and establish specification thresholds for the selection guidelines. Since stiffness calculation in the BBR test method requires that measurements be made within the linear region of viscoelastic behavior, validation of this theory was conducted for crack sealants. This was found to be generally the case with crack sealants, which allowed for the use of the time-temperature superposition. If the temperature-superposition principle is applied, the stiffness at 240s at a given temperature can be used to predict the stiffness after 5hr of loading at a temperature that is 6°C lower. With the assumption of linear viscoelastic behavior, sealants performance can be characterized through stiffness, average creep rate, and dissipated energy ratio. Stiffness was found to be sensitive to temperature changes and could be used to differentiate between sealants. The measurements of the average creep rate and the dissipated energy ratio were also found to be valuable in differentiating between sealants. In addition, numerical modeling was used to simulate the mechanical response of crack sealants at low temperatures. Parameters that may be used for evaluating crack sealant cohesive performance using the crack sealant BBR (CSBBR) are the stiffness at 240s, average creep rate, and the dissipated energy ratio. For simplicity, the first two parameters, stiffness at 240s and average creep rate, are recommended for implementation in the sealant performance grade. The recommended thresholds are maximum stiffness of 25MPa and minimum average creep rate of 0.31.

17. Key Words	18. Distribution Statement
	No restrictions. This document is available to the public through the National Technical Information Service, Springfield, Virginia 22161.

19. Security Classif. (of this report)	20. Security Classif. (of this page)	21. No. of Pages	22. Price
Unclassified	Unclassified	79	

ACKNOWLEDGEMENT

The research on the Development of Performance-Based Guidelines for the Selection of Bituminous–Based Hot-Poured Pavement Crack Sealants is sponsored by the Federal Highway Administration “pooled-fund study TPF5 (045)” and the US-Canadian Crack Sealant Consortium. The contribution of the participating states, industry, and provinces is acknowledged. This report is part of a series of reports that resulted from this study. Four reports were published by the Illinois Center for Transportation:

Al-Qadi, I.L., E.H. Fini, H.D. Figueroa, J.-F Masson, and K.K. McGhee, Adhesion Testing Procedure for Hot-Poured Crack Sealants, Final Report, No. ICT-08-026, Illinois Center for Transportation, Rantoul, IL, Dec 2008, 103 p.

Al-Qadi, I.L., E.H. Fini, J.-F Masson, A. Loulizi, K.K. McGhee, M.A. Elseifi, Development of Apparent Viscosity Test for Hot-Poured Crack Sealants, Final Report, No. ICT-08-027, Illinois Center for Transportation, Rantoul, IL, Dec 2008, 41 p.

Al-Qadi, I.L., S.-H. Yang, J.-F. Masson, and K.K. McGhee, Characterization of Low Temperature Mechanical Properties of Crack Sealants Utilizing Direct Tension Test, Final Report, No. ICT-08-028, Illinois Center for Transportation, Rantoul, IL, Dec 2008, 70 p.

Al-Qadi, I.L., S.-H. Yang, M.A. Elseifi, S. Dessouky, A. Loulizi, J.-F. Masson, and K.K. McGhee, Characterization of Low Temperature Creep Properties of Crack Sealants Using Bending Beam Rheometry, Final Report, No. ICT-08-029, Illinois Center for Transportation, Rantoul, IL, Dec 2008, 81 p.

Two internal reports on aging and sealant characterization were published by the National Research Council of Canada and a summary can be found in the following papers):

Collins, P., Veitch, M., Masson, J-F., Al-Qadi, I. L., Deformation and Tracking of Bituminous Sealants in Summer Temperatures: Pseudo-field Behaviour, *International Journal of Pavement Engineering*, Vol. 9, No. 1, 2008, pp. 1-8.

Masson, J-F., Woods, J. R., Collins, P., Al-Qadi, I. L., Accelerated Aging of Bituminous Sealants: Small-kettle Aging, *International Journal of Pavement Engineering*, Vol. 9, No. 5, 2008, pp. 365-371.

In addition, an executive summary report of the study was published by the Virginia Transportation Research Council (the leading state of the study):

Al-Qadi, I. L. J-F. Masson, S-H. Yang, E. Fini, and K. K. McGhee, Development of Performance-Based Guidelines for Selection of Bituminous-Based Hot-Poured Pavement Crack Sealant: An Executive Summary Report, Final Report, No. VTRC 09-CR7, Virginia Department of Transportation, Charlottesville, VA, 2008, 40 p.

DISCLAIMER

The project that is the subject of this report was completed under contract with the Virginia Transportation Research Council, which served as lead-state coordinator and project monitor for the partner states of Connecticut, Georgia, Maine, Michigan, Minnesota, New Hampshire, New York, Rhode Island, Texas, and Virginia. The contents of this report reflect the views of the authors, who are responsible for the facts and the accuracy of the data presented herein. The contents do not necessarily reflect the official views or policies of the Virginia Transportation Research Council, the partnering states, the Illinois Center for Transportation, the Illinois Department of Transportation, the Federal Highway Administration, or the remaining members of the Crack Sealant Consortium. This report does not constitute a standard, specification, or regulation. Any inclusion of manufacturer names, trade names, or trademarks is for identification purposes only and is not to be considered an endorsement.

EXECUTIVE SUMMARY

Crack sealing has been widely used as a routine preventative maintenance practice. Given its proper installation, crack sealants can extend pavement service life by three to five years. However, current specifications for the selection of crack sealants correlate poorly with field performance. The purpose of this research was to develop performance guidelines for the selection of hot-poured bituminous crack sealants at low temperature. In this part of the research, the creep behavior of crack sealant at low temperature is measured and performance criteria for material selection were developed. Because various pavement and State agencies are well acquainted with and own the Bending Beam Rheometer (BBR), which was developed during the Strategic Highway Research Program (SHRP), an attempt was made to utilize the same setup to test hot-poured bituminous-based crack sealants. Testing conducted in this research project indicated that the standard BBR was inappropriate for testing soft bituminous-based hot-poured crack sealant, even at -40°C. The measured deflection exceeded the BBR limit, for some sealants, after only a few seconds of loading. To address this issue, the moment of inertia of the tested beam was increased by doubling its thickness (from 6.35mm to 12.7mm). For the new beam dimensions, it was found that only 4% of the beam center deflection is due to shear, a value deemed acceptable for sealant evaluation and comparison.

In an effort towards developing a robust testing procedure, 15 sealants from various manufacturers were included in the study and tested between –4°C and –40°C. In addition, five sealants, which have known field performance, were tested to validate the laboratory results and establish specification thresholds for the selection guidelines. Since stiffness calculation in the BBR test method requires that measurements be made within the linear region of viscoelastic behavior, validation of this theory was conducted for crack sealants. This was found to be generally the case with crack sealants, which allowed for the use of the time-temperature superposition. If the temperature-superposition principle is applied, the stiffness at 240s at a given temperature can be used to predict the stiffness after 5hr of loading at a temperature that is 6°C lower.

With the assumption of linear viscoelastic behavior, sealants performance can be characterized through stiffness, average creep rate, and dissipated energy ratio. Stiffness was found to be sensitive to temperature changes and could be used to differentiate between sealants. The measurements of the average creep rate and the dissipated energy ratio were also found to be valuable in differentiating between sealants. In addition, numerical modeling was used to simulate the mechanical response of crack sealants at low temperatures. Parameters that may be used for evaluating crack sealant cohesive performance using the crack sealant BBR (CSBBR) are the stiffness at 240s, average creep rate, and the dissipated energy ratio. For simplicity, the first two parameters, stiffness at 240s and average creep rate, are recommended for implementation in the sealant performance grade. The recommended thresholds are maximum stiffness of 25MPa and minimum average creep rate of 0.31.

TABLE OF CONTENTS

FINAL CONTRACT REPORT

CHARACTERIZATION OF LOW TEMPERATURE MECHANICAL PROPERTIES OF CRACK SEALANTS USING BENDING BEAM RHEOMETRY

Imad L. Al-Qadi
Founder Professor of Engineering
Illinois Center for Transportation, Director
Department of Civil and Environmental Engineering
University of Illinois at Urbana-Champaign

INTRODUCTION

Crack sealing and filling are the most widely used maintenance activity for in-service pavements. This preventive maintenance activity is particularly favored among pavement agencies because it is inexpensive, quick, and well-proven to delay the pavement deterioration caused by other mechanisms, such as weakening of subgrade and aggregate layers through water infiltration and stripping of hot-mix asphalt (HMA) layers. Several years of service life may be added to a pavement at a relatively low cost if an appropriate sealant material is correctly installed at the right time. Several studies demonstrated the cost-effectiveness of crack sealing and filling (Joseph 1990; Cuelho et al. 2002; Cuelho et al. 2003; Fang et al. 2003; Ward 2001; Chong and Phang 1987; Chong 1990). Chong and Phang (1987) reported that crack sealing added about four years of life to flexible pavements. Chong (1990) also reported that maximum cost-effectiveness was achieved when the first treatment was performed between the third and fifth year of the pavement service life and a second treatment between the eighth and ninth year of the pavement service life.

In order to maintain a cost-effective crack sealing/filling operation and achieve the expected performance of crack sealnts, two factors must be closely controlled: quality of the installation and sealant mechanical and rheological properties (such as viscosity, bulk stiffness, and adhesive bond strength). Regardless of sealant quality, improper installation will cause premature failure and lead to a shorter service life. The installed sealant material should also have the appropriate rheological properties to adequately accommodate crack movements, particularly during the winter season. Cracks in pavements may move in both horizontal and vertical directions. Vertical movement is a result primarily of traffic loading. Because the crack may divide the pavement into two parts, differential movement between the two parts occurs when the load transfer is not full; this is usually referred to as a "working crack". Horizontal movement in a crack is primarily due to thermal expansion and contraction of the pavement. Thermally-induced movements tend to occur on a seasonal basis rather than on a daily basis (Linde 1988). Cracks open the most during winter, and tend to close during summer, and they rarely return to their original width. In fact, cracks seem to increase in width every year. In some cases, cracks were found to move a considerable amount, while in other cases; they barely moved (Linde 1988).

Existing standards and specifications in the United States and Canada describe specific test methods to measure the properties of crack sealants. Laboratory tests and specifications for crack sealant materials were established by several organizations,

including American Society for Testing and Materials (ASTM), American Association of State Highway and Transportation Officials (AASHTO), and U.S. and Canadian federal, state, provincial, and municipal agencies. Chehovits and Manning (1984) reported that eight specific properties are desirable in a product to perform adequately as a crack sealant:

1. ability to be easily and properly placed in a crack with application equipment,
2. adequate adhesion to remain bonded to HMA crack faces,
3. adequate resistance to softening and flow at high, in-service pavement temperatures so that the sealant will not flow from the crack,
4. adequate flexibility and extensibility to remain bonded to crack faces when extended at low, in-service temperatures,
5. sufficient elasticity to restrict the entrance of incompressible materials into the crack,
6. sufficient pot life at application temperatures,
7. resistance to degradation from weather to ensure long in-service life of the sealant, and
8. compatibility with HMA, and low cure time to allow traffic as soon as possible after application.

Several empirical tests exist that are thought to indicate whether a selected crack sealant material possesses the required properties. ASTM Standard D5329-04 (Standard Test Methods for Sealants and Fillers, Hot-Applied, for Joints and Cracks in Asphaltic and Portland Cement Concrete Pavements) summarizes most of these tests. These include non-immersed cone penetration, fuel-immersed cone penetration, the flow test, the non-immersed bond test, the water-immersed bond test, the fuel-immersed bond test, the resilience test, the oven-aged resilience test, the asphalt compatibility test, the artificial weathering test, the tensile adhesion test, the solubility test, and the flexibility test.

These tests are used by most state highway agencies in selecting their crack sealing materials; but the specification limits may vary from one state to another. These differences create difficulties for crack sealant suppliers because many states with the same environmental conditions specify different limits for the measured properties. These tests were also reported to poorly characterize the rheological properties of bituminous-based crack sealants and to predict sealant performance in the field. This may lead to premature sealant failure when used in unfavorable conditions.

The inability of current ASTM and AASHTO standard tests to provide a good indication of field performance has been repeatedly documented in the literature (Belangie and Anderson 1985; Smith and Romine 1999; Masson et al. 1999; Masson 2000). The main reason that current specifications poorly predict field performance is that these tests are empirical and that the measured parameters are not based on any rheological properties. Therefore, it has been a common practice to evaluate the performance of sealing materials through field trials. However, even the results from field tests are sometimes controversial because a sealant can perform well at one site and fail in another, simply because of differences in environmental or installation conditions. Masson and Lacasse (1999) showed that current ASTM specifications for selecting hot-poured crack sealants are based on tests whose results are not correlated with field performance.

PURPOSE AND SCOPE

The main objective of this project was to develop laboratory tests that measure bituminous-based crack sealants rheological properties, which may improve the selection of sealant materials. Ultimately, the aim was to predict crack sealant performance at a

particular site, with a benefit of being able to select durable sealants. Special attention was given to make use of the equipment originally developed during the five-year Strategic Highway Research Program (SHRP), which were used to measure binder rheological behavior as part of the performance grade (PG) system. At low temperatures, the SHRP BBR was modified and used to predict the cohesive performance of crack sealants. This report describes the research tasks conducted to achieve the objectives of this phase of the study. This included the following research tasks:

- Development of modifications to the binder BBR test setup and specimen preparation originally developed by SHRP.
- Validation of the time-temperature superposition principle for crack sealants and verification of the applicability of the linear viscoelastic theory for these materials at low temperature.
- Evaluate the effect aging process on crack sealants rheological behavior.
- Identification of laboratory-measured parameters to predict the cohesive field performance of crack sealants at low temperature and recommend related thresholds.

METHODS

The key to improving sealant durability is to develop effective performance guidelines for selection and application of sealants. Acknowledging the deficiencies of the current specification system, more than 26 State and Province departments of transportation, manufactures, cities, and research agencies in North America have partnered to develop performance-based guidelines for the selection of bituminous-based hot-poured crack sealants. A major milestone of this project was to make use of the well-established methods and equipment originally developed during the five-year Strategic Highway Research Program (SHRP) as part of the Performance Grade (PG) system for asphalt binders. Because the equipment utilized in this system is already owned by various pavement and State agencies, this was an attractive and economical choice that was adopted by this research project.

Previous researchers have attempted to test crack sealant using the SHRP bending beam rheometer (BBR); but because of the high flexibility of crack sealants and the large deformation experienced under loading, it was concluded that this equipment was not suitable for measuring the stiffness of these materials (Zanzotto 1996). Therefore, in order to use the equipment developed by SHRP, some modifications were needed to allow for testing hot-poured sealants. The proposed modifications were validated and recommended performance parameters, to characterize creep behavior of hot-poured bituminous-based crack sealants at low temperature using the CSBBR, were suggested.

Crack Sealant Bending Beam Rheometer (CSBBR)

This section presents the results of laboratory tests used to evaluate the application of the SuperPave™ BBR for testing of crack sealants. This ultimately led to a series of modifications to address the rheological differences between asphalt binder and crack sealant. The modified equipment is referred to as the Crack Sealant Bending Beam Rheometer (CSBBR).

SuperPaveTM Bending Beam Rheometer

Research conducted in the late 1960s and early 1970s suggested that binder stiffness and thermal cracking in flexible pavements are closely correlated, after a loading time ranging from 3,600 to 20,000s (Hills and Brien 1966; Readshaw 1972). Based on this correlation, researchers suggested limiting the creep stiffness at 200MPa after a loading time of 2hr. Based on these field observations, the SuperPave™ BBR testing protocol imposed upper limit on the measured creep stiffness. However, for practical reasons and assuming the time-temperature superposition principle is valid, loading time in the BBR was reduced from 2hr to 60s while raising the temperature by 10°C. In addition, the maximum allowable creep stiffness was changed from 200 to 300MPa as the original threshold was judged overly restrictive (Anderson et al. 1994). After several preliminary tests, the total loading time of 240s was selected. This loading time provided a sufficient time span to create an overlap between the different creep curves when it is beneficial to construct master curves spreading over several orders of time magnitude (Bahia and Anderson 1995).

In addition to the creep stiffness, the stress relaxation ability of the asphalt binder was also considered and measured from the creep rate, also known as the m-value. The m-value is the slope of the log stiffness versus log time curve at any time, t. Physically, a higher creep rate (m-value) would indicate a faster relaxation of stresses, which is desirable at low temperature. By applying a constant load to the asphalt beam and measuring the center deflection of the beam throughout a timed test procedure, the creep stiffness (S) and creep rate (m) can be calculated. The creep load simulates the thermal stresses that gradually build up in a pavement when the temperature drops. Based on elementary beam theory, the deflection of a prismatic beam in a three-point bending mode can be calculated using the following equation:

$$\delta = \frac{PL^3}{48EI} \qquad (1)$$

where,

P = constant applied load (N);
L = span length (102mm);
δ = deflection of the beam at midspan (mm);
E = modulus of elasticity (N/mm^2);
I = moment of inertia (mm^4) = $bh^3/12$.
b = beam width (12.7mm); and
h = beam thickness (6.35mm).

The selected beam dimensions (b, h) meet the requirements for applying the elementary beam theory by keeping the shear effects on the center deflection minimal (less than 1%). For this beam configuration, the span to depth ratio was 16/1, and the depth to width ratio was ½. A major simplification, which was introduced to calculate creep stiffness, assumed that asphalt binder behaves as a linear viscoelastic material. This assumption was evaluated and validated by Marasteanu and Anderson (2000). Using the elastic-viscoelastic correspondence principle, the creep stiffness was then calculated as follows:

$$S(t) = \frac{PL^3}{4bh^3\delta(t)} \quad (2)$$

where,

S(t) = time-dependent stiffness.

As shown in the previous section, several critical assumptions were made in the analysis of the data obtained from the BBR. Before adopting this equipment for testing bituminous hot-poured sealants for cracks and joints, it is essential to ensure that these assumptions are applicable for crack sealants. Obviously, although there is similarity between asphalt binder and hot-poured crack sealants, some differences exist between the two materials. In fact, hot-poured crack sealants behave similarly to highly modified asphalt rubber.

The first assumption in the SuperPave™ specification system is that all the measurements are made in the linear region of viscoelastic behavior. If the measurements are not taken at relatively narrow strain amplitudes, this assumption will not be valid. A departure from the linear region of behavior would necessitate a highly complex analysis to calculate the stiffness of the material, and would mean that the suggested analysis would bear no resemblance to the existing SuperPave™ binder specification system other than using similar equipment. Therefore, measurements need to be checked for being obtained in the linear region of viscoelastic behavior. The check of linearity suggested by Marasteanu and Anderson (2000) was adopted in this study.

Another critical assumption made in the SuperPave™ specification system is that the stiffness after two hours of loading can be approximated by the stiffness after 60s of loading by raising the temperature by 10°C. It was recently reported that this assumption was never validated experimentally in the SHRP program by actually conducting the 2-h tests. Moreover, recent evaluation of this assumption by Basu and his colleagues indicated that this hypothesis was not correct (Basu et al. 2003). Results of this study indicated that the 60s stiffness values were significantly higher than the 2-h stiffness values and that the differences in stiffness ranged from 32 to 66% depending on the binder type.

A third assumption made in the SuperPave™ specification system was that the selected conditioning time of one hour is sufficient to reduce the effect of physical hardening on the measured stiffness. During the SHRP program, it was noticed that asphalt binders exhibited a significant hardening that resulted in a sharp increase in the material's stiffness. This phenomenon increased sharply in the first 24h, and then stabilized to become negligible after 3 to 7 days. Although the SHRP program did not thoroughly quantify this factor, a standard conditioning time of one hour was decided so that hardening could be discounted. Such selection would need to be validated for crack sealant materials.

The final assumption made in the SuperPave™ specification system was that the creep stiffness and the slope of changing stiffness (m-value) would suffice to distinguish and grade the low temperature performance of different binders. This is a critical assumption that was investigated by various researchers (Anderson et al. 1994; Hesp, 2004). Based on the results of these studies, it was concluded that the original specification did not accurately reflect the low temperature performance of binders.

Bending Beam Rheometer Equipment Evaluation and Test Modification

While attempt to use SuperPave™ BBR to test crack sealants, several problems have encountered. The first problem was that the AASHTO TP1-97 binder sample

preparation procedure was followed to evaluate the potential use of this practice for bituminous hot-poured crack sealants. However, although this AASHTO procedure recommends using Mylar strips to prevent the binder adhering to the mold, the technique was not effective with crack sealant materials, as they tended to stick to the mold during de-molding. Several release agents (e.g., a mix of glycerin and talc) were tried, with silicone grease found to work best with crack sealant materials. The second problem encountered during the testing was the relatively soft crack sealant material. Due to the excessive softness of the crack sealant, several tested sealants were too soft to measured by the SuperPave™ BBR. The specimen quickly deformed within the 240s testing period. To overcome this issue, the specimen thickness was doubled. The third problem was the relatively high variation in testing results. Crack sealant has much more complex composition compared to asphalt binder. Crack sealant may have high content of polymer, crumb rubber particales, lime, and/or filler. This makes sealant more viscos material compared to asphalt binder and its inhomogeneity becomes a major issue during the sealant pouring into the mold. To overcome this problem, each specimen was poured from individual container, which contains the same amount of sealant sample. This improves the test repeatability significantly.

Time-Temperature Superposition Principle Verification at Low Temperature

The SuperPave™ specifications for asphalt binder assume that creep responses are measured in the linear region of its viscoelastic behavior. In order for the time-temperature superposition principle to be valid, measurements must be taken at relatively narrow strain amplitudes. Therefore, it is essential to ensure that crack sealants measurements are obtained in the linear region of viscoelastic behavior. Al-Qadi et al. (2006) and Elseifi et al. (2006) have studied quantifying the linear response of sealant materials. The studies utilized two conditions to verify the linearity as suggested by Marasteanu and Anderson (2000). Marasteanu and Anderson (2000) showed that for a linear viscoelastic material, time response measurements should be independent of the applied stress level, and second, the linear superposition principle should be applicable to a sequence of loading and unloading cycles. Therefore, creep loading at 250, 490, and 980mN was conducted on sealant.

Effect of Aging

When sealant is subjected to weathering, the stiffness of the sealant varies depending on the chemical composition of the material. Hence, it is important to simulate the effects of aging on sealants because their mechanical properties can be altered from their original state. Sealant aging is typically divided into two categories: short-term aging, which occurs during the installation process, and long-term aging, which occurs after construction, primarily due to climate exposure and loading.

Currently, there is no method to simulate hot-poured bituminous crack sealant aging. Aging effects are usually accounted for by subjecting sealant to simulated aging then measuring its mechanical properties by conducting standard physical tests (such as viscosity, dynamic shear rheometer test, BBR test, and the direct tension test). In this study, vacuum oven aging (VOA) was used to simulate the aging and weathering of crack sealants during installation and service.

In this procedure, developed by Masson et al. (2007) as part of this project, the homogenized sealant is cut into slices and then placed in a stainless steel pan in a heated oven in order to achieve a film thickness of less than 2mm. The sealant is then removed from the oven and allowed to cool down at room temperature before enduring accelerated aging in the VOA, which is preheated to 115ºC. The sealant is then transferred into the vacuum oven for 16hr under a vacuum of 760mm of mercury. After this period, the steel pan is placed back into a regular oven at 180°C and heated until the sealant is sufficiently fluid. The sealant from each pan is poured into individual containers, which ensures the homogeneity of the sealant for future performance testing. Through chemical analysis, this procedure was shown to be suitable for aging of bituminous crack sealants. It does not cause significant degradation of polymer constituents nor excessive oxidation.

The aging process was first conducted with Precision vacuum oven model 29 (Figure 1a a). However, a study was conducted to measure the internal temperature distribution in the vacuum oven and showed that the temperature distribution within the oven can be as high as 25°C between the upper and lower shelves. Therefore, a new vacuum oven from Sheldon lab model 1445 (Figure 1b) was used and the measurement showed that a relatively uniform temperature distribution can be achieved when a special design shelves were used in this oven. The special shelves had a height of 23mm and therefore uniform temperature distribution can be reached at the middle portion of the oven. Therefore, all the sealants used in the study were aged in the Sheldon lab vacuum oven prior to testing.

(a) (b)

Figure 1. Vacuum Oven Used for Aging the Sealant Material (a) Precision Vacuum Oven and (b) Sheldon Vacuum Oven

Bituminous-Based Crack Sealant Types and Identifications

In general, sealants are composed of base bituminous, styrene-butadiene copolymer, and filler. The styrene-butadiene (SB) copolymer consists of linked blocks of polystyrene (PS) and polybutadiene (PB). The fillers may include crumb rubber block, rubber powder, and fibers. The variety of chemical compositions for crack sealants can significantly influence their rheological properties. Therefore, 25 sealants with varying chemical compositions were selected for this study to validate the developed testing procedure using the Crack Sealant BBR (CSBBR). These sealants represent a wide array of rheological behaviors and they are expected to be used in various locations in North America. Variations in the rheological properties can be attributed to different factors including the

source of the origin crude, the refining and modification process, and the content of polymer, filler, and additives.

Sealant products used at University of Illinois were designated by a two-character code, which identifies the sealant type (Error! Reference source not found.). Those sealants with one character code are those sealants, which were included in the field trials conducted in Canada. The field sealants were installed in the early 1990s, and were sampled in the un-aged (V) condition and after 1 (w1), 3 (w3), 5 (w5), and 9 (w9) years of weathering. For example, sealant A was installed in Montreal, Canada in 1990. During sealant installation, portions of the virgin sample were cut and designated as A_V. A virgin sealant that was aged in the laboratory according to the acceleration aging procedure developed by NRC Canada is designated as A_AV. Field samples of sealant A were taken at year 1, 3 and 5 years after installation and they were designated as A_w1, A_w3, and A_w5. On the other hand, although the field performance of some of the selected sealants was not known; they provided a wide array of rheological behaviors ranging from very soft to very stiff crack sealants.

Table 1. Sealants Description and Designation

ID	Notes	Penetration	Flow	Resilience
		25°C (dmm)	60°C (mm)	25°C
QQ	Stiffest crack sealant	22	0	36
EE	Expected high temperature grade is -22°C	47	0	51
ZZ	Used in San Antonio, TX	42	N/A	N/A
YY	Used in San Antonio, TX	42	N/A	N/A
AB	Used in San Antonio, TX	40	N/A	23
VV	Modified with fiber	N/A	N/A	N/A
UU	Used by SHRP H106	62	1.5	N/A
AE	Widely used in NY, VA, and NH	N/A	N/A	N/A
DD	Expected low temperature grade is -34°C	80	1.5	50
MM	For aging study	120	1	70
WW	Field data available	N/A	N/A	N/A
NN	Field data available	75	0	70
AD	SHRP H106 field data available	N/A	1	80
PP	Field data available	130	1	44
BB	Softest crack sealant	148	0	80
SS	For preliminary testing	122	0.1	63
CC	Field data available	N/A	0	65
GG	For preliminary testing	66	0	75
HH	SHRP H106 field data	N/A	0	44
A	Field data available	86	0.5	57
B	Field data available	68	0.5	64
C	Field data available	78	0	59
E	Field data available	124	1	73
G	Field data available	50	0.5	51
J	Field data available	66	6	48

Cohesive Performance at Low Temperature – Laboratory Parameters

Crack Sealant Stiffness

The rational for measuring stiffness of crack sealant is different than that for asphalt binder due to their different function in the pavement system. A crack sealant needs to be flexible enough to deform while the crack opens. Therefore, the strength of crack sealant is not the primary concern. Instead, the sealant flexibility, extendibility and stress relaxation are the important parameters. In contrast, asphalt binder holds the aggregates together to provide the structure strength. In order to decide on the critical loading time for crack sealant material at low temperature, temperature history at several locations in the US was reviewed.

Figure 2a presents the daily temperature variation in International Falls, Minnesota (one of the coldest locations in the US) during the winter season; the data obtained from files for the typical meteorological year (TMY). These data represent temperatures judged to be typical based on a statistical analysis of 30 years of weather records. As shown in this

figure, the temperature drops over 10h, between 4PM and 2AM, to stabilize at its lowest level of -27°C for about 7hr during the night. It is worth noting that in several Canadian cities that were part of this project, the temperature could reach lows of -40°C in the winter. Figure 2b presents the average daily temperature variation in a much warmer location: Roanoke, Virginia, during winter. In this location, the temperature drops over about 6hr and it is stable at the low of -1°C for about 3hr. Hence, with dropping temperatures, sealants may be under tensile strain for 6 to 10hr. With constant temperatures and static cracks and joints, the internal stresses may be dissipated by the relaxation of stress over 3 to 7 hrs.

Figure 3 presents the constructed master curve for sealant YY at -4°C, -10°C, and -16°C. The master curve makes it possible to determine the stiffness after 5hr of loading at a reference temperature of -16°C. At the same temperature, the reduction in stiffness after 5hr of creep loading is significant and ranges between 70% and 80% of the calculated stiffness at a loading time of 240s. If the temperature superposition principle is applied, the stiffness at 240s for a given temperature can be used to predict the stiffness after 5 hrs of loading at a temperature of approximately 12°C. Given the variation in sealant response to temperature change, 6°C shift is deemed appropriate.

As previously discussed, the rationale used for setting a maximum threshold limit for the stiffness of crack sealants is different than its use for asphalt binders. A maximum value for stiffness must be set to ensure the flexibility of crack sealant at low temperature after 5hr of creep loading.

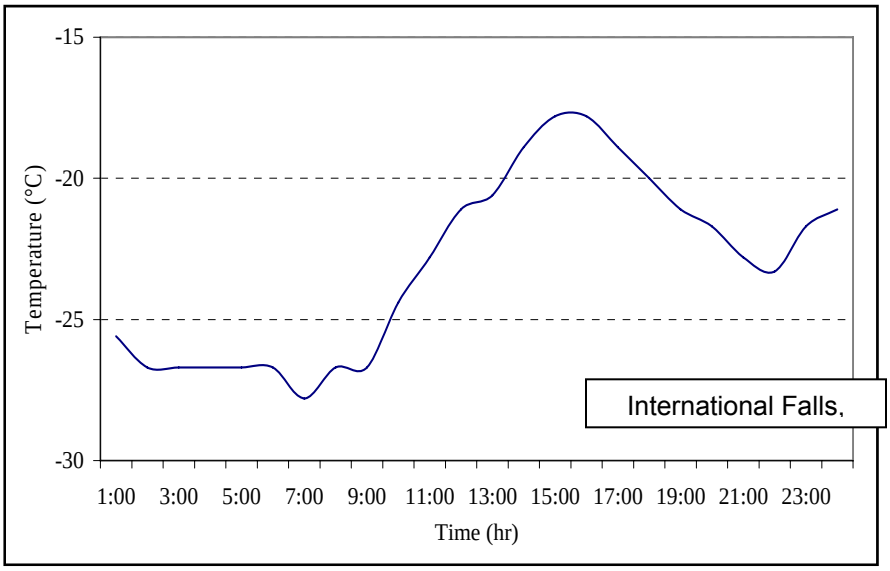

(a)

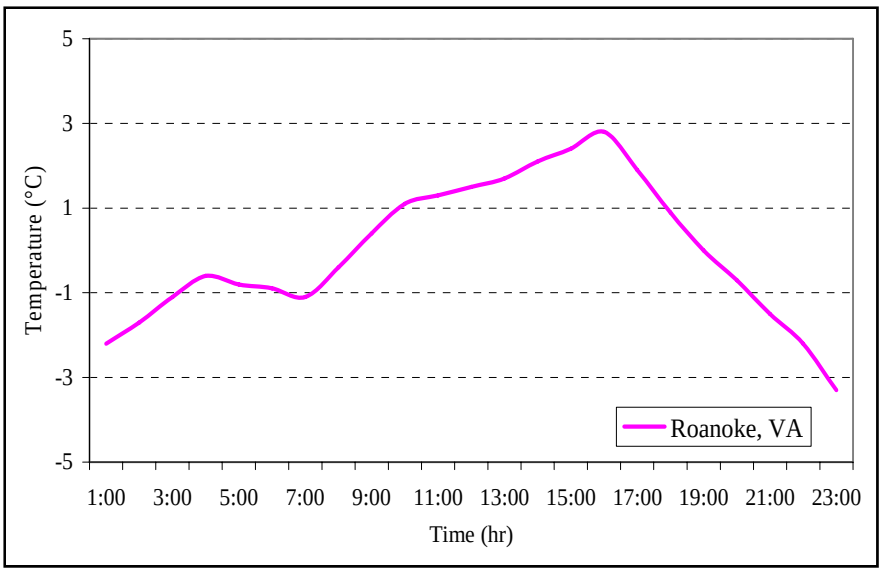

(b)

Figure 2. Variation of Air Temperature for Two Locations: (a) International Falls, MN, and (b) Roanoke, VA

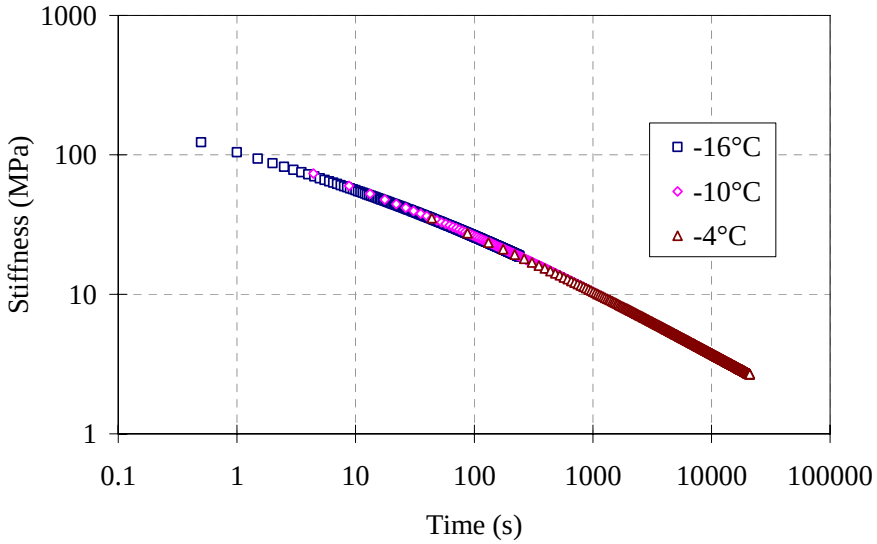

Figure 3. Construction of a Master Curve for Sealant YY from the BBR Test Data Obtained at Three Temperatures

Average Creep Rate

Another method to evaluate the creep behavior from CSBBR data is to determine the average rate of creep and recovery. The creep data versus time were fitted to a power law model. The exponents of the power law model represent the average creep rate. The absolute values of the exponents were then compared. The calculation of the average creep rate for sealant NN at -40°C is illustrated in Figure 4. From the results presented in these figures, it can be estimated that the average rate of creep is 0.34.

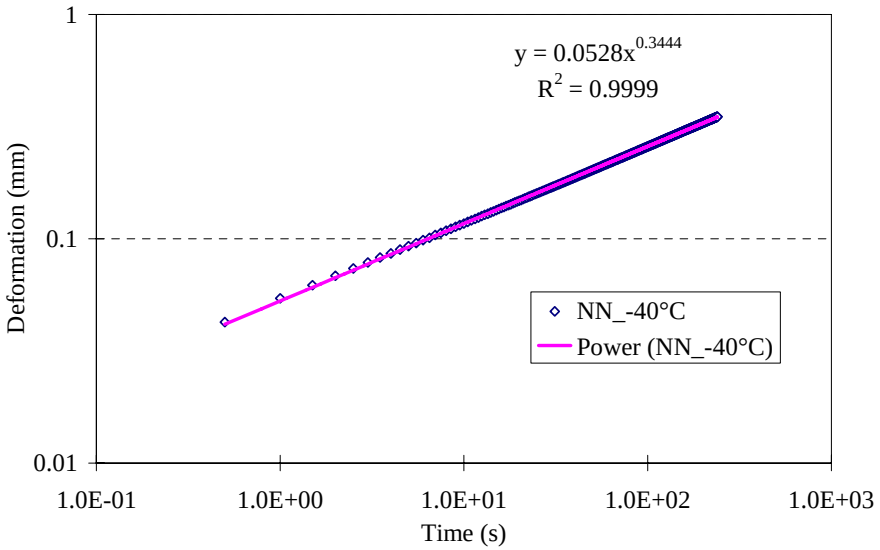

Figure 4. Average Creep Rate for Sealant NN at -40°C

Dissipated Energy Ratio

Another indicator considered in this study was the dissipated energy ratio for the sealant during the loading phase. The ratio for dissipated energy reveals the proportion of elasticity and viscosity of the material. A two-term Prony series model was used to investigate the viscoelastic nature of the sealant. The relationship between strain, , and stress, , can be expressed by the compliance, D(t)= / . The Prony series model describes the creep compliance as follows:

$$D(t) = \frac{1}{E_0} + \frac{1}{E_1}(1 - e^{-(t/\tau_1)}) + \frac{1}{E_2}(1 - e^{-(t/\tau_2)}) \qquad (3)$$

where,
D(t) = is the tensile creep compliance at time t;
E_1, E_2 = material constants; and
τ_1, τ_2 = retardation time.

The parameters of the Prony series are time-independent variables relative to the creep modulus or compliance. Hence, the output of the CSBBR test data was first converted to compliances and Prony series parameters were calculated for each test run by fitting the measured compliance to the Prony series model using regression analysis. Figure 5 presents a comparison between measured versus model plot. Since the model fairly fits the experimental data, the Prony series parameters were then used to calculate dissipated and stored energy for each sealant. Equations (4) and (5) present the stored and dissipated energy calculations, respectively (Johansson and Isacsson 1998). The dissipated energy ratio is calculated as $W_{dissipated}/W_{stored}$.

$$W_{store} = \frac{\sigma_0^2}{2}\left[\frac{1}{E_0} + \frac{1}{E_1}(1 - 2e^{-(t/\tau_1)} + e^{-(2t/\tau_1)}) + \frac{1}{E_2}(1 - 2e^{-(t/\tau_2)} + e^{-(2t/\tau_2)})\right] \qquad (4)$$

$$W_{dissipated} = \sigma_0^2 \left[\frac{1}{2E_1}(1 - e^{-(2t/\tau_1)}) + \frac{1}{2E_2}(1 - e^{-(2t/\tau_2)}) \right] \quad (5)$$

where,

W= energy per volume;

t = maximum loading time (240s); and

σ_0 = stress in outer fiber at mid-span and calculated as follows:

$$\sigma_0 = \frac{3PL}{2bh^2} \quad (6)$$

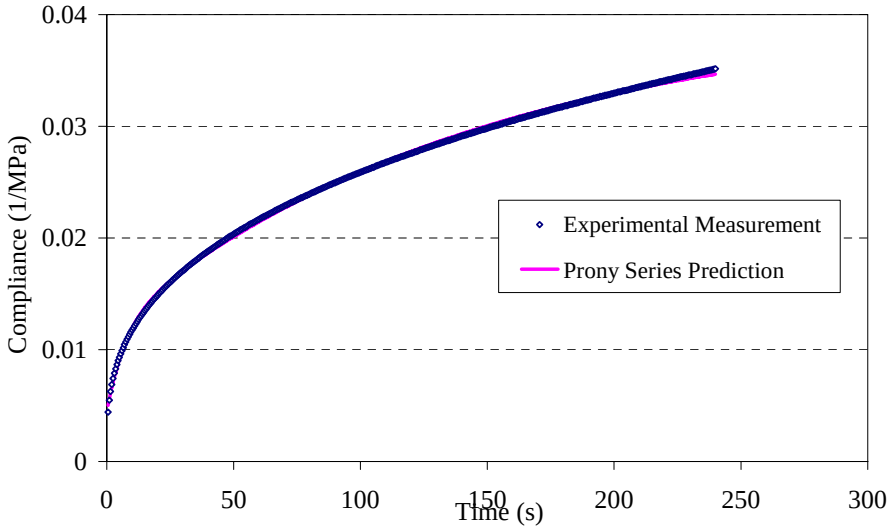

Figure 5. Comparison of Measured versus Model Plot Data for Sealant NN at -40°C Fitted with a Two-Term Prony Series Model

Viscoelastic Behavior and Modeling

The extensive modification used in producing hot-poured crack sealants results in two major differences at low service temperature when compared to asphalt binders. First, at low service temperature, crack sealants may not be in a glassy state, with a glass transition temperature (T_g) reaching as low as -78°C for a very soft sealant such as PP (as measured in this study). Hence, a crack sealant may not experience pure fracture as it is usually encountered in asphalt binders. It is well known that in the glass transition region, a material is brittle and only a small portion of the molecules is in motion or responsive to the applied load. This results in the material responding elastically and linearly to the load. With such a low glass transition temperature, soft sealants may behave as viscoelastic even at low service temperatures (i.e., -4 to -40°C). In fact, the cohesive failure of the soft sealant at low temperature may be attributed to imperfection at the interfaces between the different sealant components rather than to a clear fracture of the material.

Second, in contrast to the single-event thermal cracking considered in the SuperPave™ binder specification system, cohesive failure of crack sealants is a progressive, localized damage process due to fluctuating stresses and strains in the material and a buildup of irrecoverable deformations. Therefore, the material response under cyclic thermal loading is of particular interest.

Evaluating the mechanical behavior of crack sealants at low temperature has usually focused on either experimental or laboratory approaches. Since a closed-form solution is not available for a pavement structure incorporating a sealed crack, the mechanical analysis of this problem may only be achieved using numerical methods and has usually been overlooked in the literature. Although recent work has been presented to evaluate joint seals using finite element (FE) models, researchers have reported difficulties in adopting an accurate constitutive model to describe the mechanical behavior of crack sealants (Khuri and Tons 1993). Reported difficulties include tedious testing procedures and inaccuracy of available models. With the development of a simple creep test at low temperature using the CSBBR test setup, a linear viscoelastic model is presented to describe the mechanical response of crack sealants. This response behavior was further studied utilizing the Kelvin-Voight viscoelastic model simulation. The availability of such a constitutive model would allow for an accurate determination of in-situ crack sealant responses to thermal and traffic loading.

Mechanical Response of Hot-Poured Bituminous-Based Crack Sealant

Bituminous crack sealant is a typical viscoelastic material, which exhibits elastic (solid-like) and viscous (fluid-like) mechanical behavior. The elastic response is completely recoverable and it is generally only a small portion of the total response. The viscous portion, which dominates the behavior, dissipates all work energy applied to the material due to the flow within the material (Figure 6). The viscoelastic response due to creep loading is conclusively affected by the percentage of polymers and crumb rubber, which varies in each sealant. In order to fully utilize numerical methods, such as FE analysis, to describe crack sealant behavior, it is important to first characterize the material's rheological properties using adequate constitutive models. It is also of utmost importance that the utilized models are capable of describing the material's behavior in order to be incorporated into a numerical presentation.

To predict the performance of hot-poured crack sealants, it is necessary to describe its stress-strain relationship. Viscoelastic theory describes a material's constitutive stress-strain relationship that requires time to respond to the imposed excitation (delayed response). When the stress is proportional to the strain at any given frequency and temperature, the material is termed linear viscoelastic. Upon application of a small excitation and depending on the applicable temperature and loading frequency, many materials may be assumed to behave in the linear viscoelastic region. The use of linear viscoelastic theory is somewhat simpler when compared to the use of nonlinear viscoelastic theory, which requires extensive testing for a material's constitutive behavior to be described.

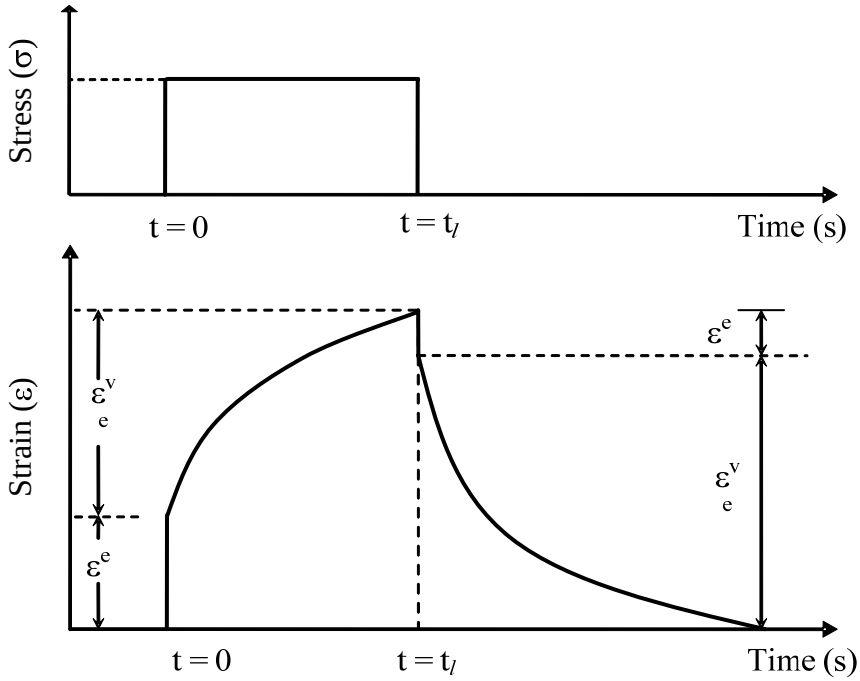

Figure 6. Schematic Representation of the Various Strain Components in an Elasto-Viscoelastic Material

Viscoelastic material properties, including creep compliance as a function of time, are determined from laboratory tests. A curve-fitting function can then be used to describe the linear viscoelastic response with a constitutive equation. Among many candidate models to describe the broad behavior of viscoelastic materials, the Prony series function may be used to fit the creep response, and is mathematically efficient when compared to other models. It has been successfully used for analytical representation of viscoelastic functions of bituminous materials (Park and Kim 2001; Lundström and Isacsson 2004; Kim and Little 2004; Elseifi et al. 2006). It is known as the generalized Voigt model, comprising linear springs and dashpots connected in a particular fashion (Findley et al. 1976). The method described in this report fits a Prony-series expansion to the response of crack sealants obtained from creep testing results. The tests were conducted using the CSBBR setup.

Kelvin-Voigt Viscoelastic Model

The stress-strain behavior of linear viscoelastic materials closely resembles that of models built from discrete elastic (spring) and viscous elements (dashpot) as shown in Figure 7. Of these two basic elements, various models (e.g., Maxwell and Kelvin elements) can be built to describe the viscoelastic response of the material to a given excitation. Testing results are commonly used to verify the applicability of a specific model to predict the performance or behavior of the material under evaluation. To describe the isotropic viscoelastic behavior of hot-poured crack sealants, a generalized Kelvin-Voigt model, which consists of a spring and dashpot connected in series, was selected for this study. In the case of a viscoelastic solid, the creep compliance at time t of a Generalized Kelvin model is given as follows (Park and Shapery 1999):

$$D(t) = D_0 + \sum_{i=1}^{K} D_i (1 - e^{-t/\tau_i}) \quad (7)$$

where,

D(t) = tensile creep compliance at time t;
D_i = material constants; and
τ_i = retardation times.

Equation (7) is also known as a Prony series expansion, and it represents a series of decaying exponentials (Figure 7). Upon applying a load, the excitation, the individual spring placed at the start of the chain (first term in Equation [7]) responds instantly. In contrast, the spring and the dashpot of the different Kelvin elements exhibit constrained motions as they are restrained to experiencing the same strain at any given time. The retardation times are generally used to provide an indication of the amount of time required for a certain component of the material (e.g., polymer) to respond to the imposed creep load. Each retardation time contributes to the fitting of the model in one order of time magnitude and is associated with a component of the material responding to the load. The number of terms in the Prony-series should not be greater than the number of logarithmic decades covered by the span of the test. For example, if a creep test is conducted for 1000s, the number of Prony series terms should not exceed three.

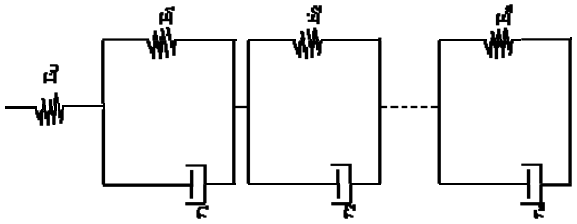

Figure 7. Mechanical Representation of a Prony Series to Describe a Viscoelastic Solid

It is assumed that all measurements are made in the linear region of viscoelastic behavior, analogous to the SuperPave™ specification system. The stiffness $E(t)$ of a linearly viscoelastic solid can be expressed as follows:

$$E(t) = E_\infty + \sum_{i=1}^{K} E_i e^{-t/\rho_i} \quad (8)$$

where,

E_∞ = equilibrium modulus;
E_i = material constant commonly referred to as relaxation strengths; and
ρ_i = relaxation time.

The glassy compliance represents the short-term behavior (t□0) of the compliance, while E_∞ represents the long-term behavior of the modulus. To facilitate the numerical implementation of a Prony series, Equation (8) can be given in a normalized form as follows:

$$\frac{E(t)}{E_o} = 1 - \sum_{i=1}^{K} \zeta_i \left(1 - e^{-t/\rho_i}\right) \quad (9)$$

where,

ζ_i = ratio between relaxation and initial modulus.

To evaluate the Prony series parameters, the three-point CSBBR test was conducted. By applying a constant load to the sealant beam and measuring the center deflection of the beam throughout the test, the creep compliance (D) can be calculated. According to the beam theory and the elastic-viscoelastic correspondence principle, the creep compliance at time (t) can be calculated as follows:

$$D(t) = \frac{\varepsilon(t)}{\sigma} = \frac{4bh^3\delta(t)}{PL^3} \quad (10)$$

where,

D(t) = time-dependent creep compliance;
σ = constant applied stress;
ε(t) = time-dependent strain;
P = constant applied load (980 mN);
L = span length (102 mm);
b = beam width (12.7 mm);
h = beam thickness (12.7 mm); and
δ = beam deflection at midspan in mm.

While Prony series parameters are normally calculated using the shear modulus data, the resulting creep compliance recorded by the CSBBR can be converted to stiffness using the convolution integral principle:

$$\int_o^t D(t)\ E(t-\psi)\ d\psi = t \quad (11)$$

Applying Laplace transform to Equation (11), the following equation can be obtained:

$$\overline{D}(s)\ \overline{E}(s) = \frac{1}{s^2} \quad (12)$$

where,

$\overline{D}$ and $\overline{E}$ = Laplace transformations of D and E, respectively; and

s = a Laplace variable.

Schapery and Park (1999) proposed a simplified technique to solve for E(t) as follows:

$$\overline{D}(s) = \frac{\Gamma(1+n)}{s} D(t)$$
$$\overline{E}(s) = \frac{\Gamma(1-n)}{s} E(t) \quad (13)$$

where,

$\Gamma(n)$ = gamma function; and

n = log-log slope of the compliance as a function of time $\frac{d(\log D)}{d(\log t)}$.

By applying inverse Laplace and substituting Equation (13) into Equation (12), the relation between the creep and stiffness moduli can be expressed as follows:

$$D(t)\ E(t) = \frac{1}{\Gamma(1+n)\Gamma(1-n)} = \frac{\sin(n\pi)}{n\pi} \quad (14)$$

At low temperatures, materials exhibit nearly ideal elastic behavior or behave as a viscoelastic solid. Thus, the relaxation shear modulus G(t) can be expressed using the elastic theory in the following form:

$$G(t) = \frac{E(t)}{2(1+\nu)} \quad (15)$$

where,

ν = a time-independent Poisson's ratio.

The stiffness modulus calculated from Equation (14) was fitted into Equation (9) to evaluate the Prony series parameters, ζ and ρ. These parameters were also implemented into FE to simulate the deflection response of a sealant as it undergoes creep loading.

Three-Dimensional Finite Element Model

The commercial software ABAQUS version 6.5 was used for FE modeling of crack sealant viscoelastic behavior. Nine-node continuum brick elements, which are appropriate for bending behavior, were used to develop a 3D FE model for the crack sealant beam with a square cross-section of 12.7mm. Figure 8a shows the geometric layout of the 3D FE model, which matches the CSBBR beam dimensions. Because the concentrated load in the CSBBR covers the width of the beam, an equivalent pressure was applied at midspan in the FE beam for a total load of 980mN. The lower end-edges were restrained in both the horizontal and vertical directions to account for the end supports in the CSBBR device frame.

Loading is applied in two stages: 980mN for 240s, followed by 30mN for 480s. Although 3D analysis was used, the model took only a few minutes to run because of its simplicity.

The normalized-fitting Prony series parameters, computed in Equation (9), were implemented in the FE for each sealant type at corresponding temperatures. To monitor the variation of the deflection with time, quasi-static analysis was conducted, which considers the time-dependent response of the material; but does not consider the dynamic response of the system, which in this analysis can be neglected. Figure 8b illustrates the model layout after the creep load was applied for a total time of 240s; while Figure 8c illustrates the horizontal stresses.

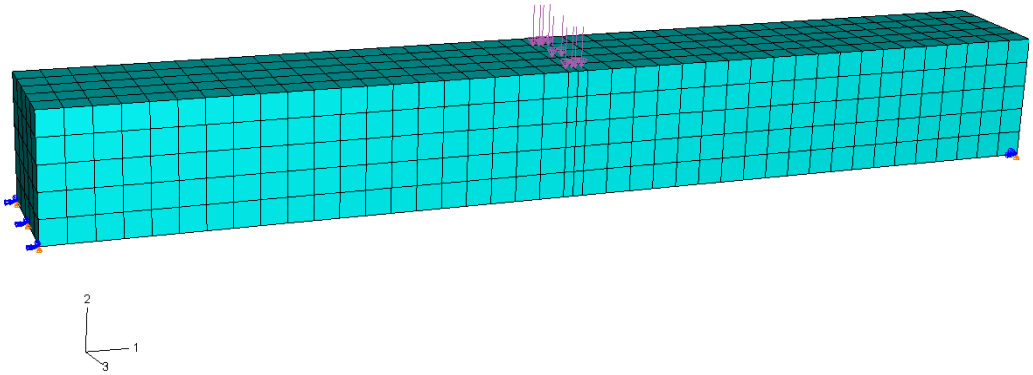

(a)

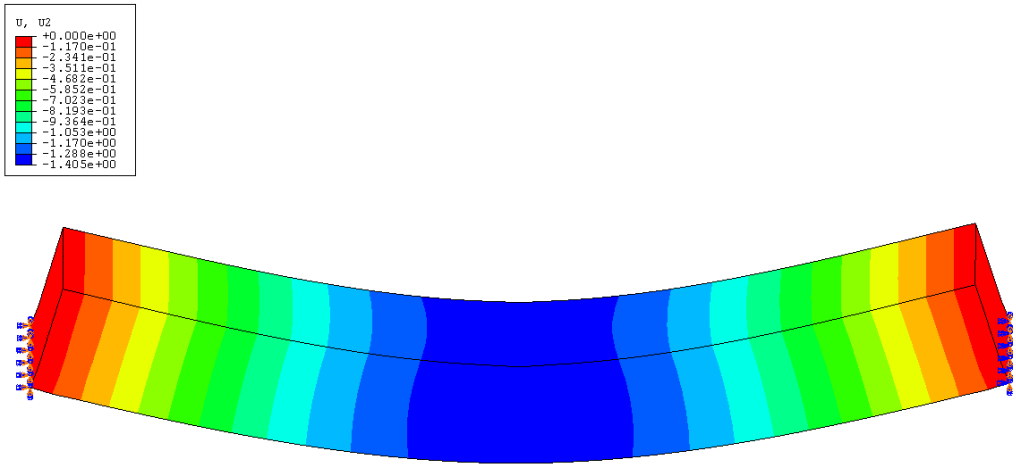

(b)

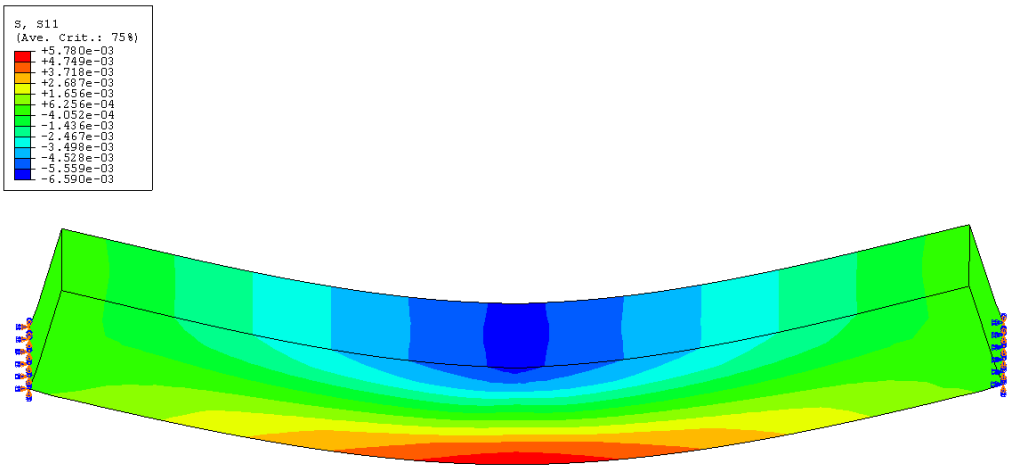

(c)

Figure 8. (a) General Description of the FE Model; (b) Vertical Displacement Distribution after 240s Creep Loading; and (c) Horizontal Stress Distribution after 240s Creep Loading

Experimental Design

Fifteen sealants were selected to test at various temperature ranges from +2°C to -40°C. This temperature range covered most of the areas in the Northern America. Each sealant was tested at three temperatures. The selection of testing temperatures is based on the manufacturers' recommended service temperatures. Sealants were further tested at +/- 6°C of the recommended service temperatures. If the recommended service temperature of the sealant is -40°C, the sealant was tested at -28°C, -34°C, and -40°C. Table 2 shows the experimental factorial design of the test.

Table 2 Experimental Factorial Design of the CSBBR Test

Temperature (°C)	2	-4	-10	-16	-22	-28	-34	-40
Sealants	QQ	QQ	QQ					
		EE	EE	EE				
		ZZ	ZZ	ZZ				
		YY	YY	YY				
		AB	AB	AB				
			VV	VV	VV			
			UU	UU	UU			
					AE	AE	AE	
						DD	DD	DD
						MM	MM	MM
						WW	WW	WW
						NN	NN	NN
						AD	AD	AD
						PP	PP	PP
						BB	BB	BB

RESULTS AND DISCUSSION

Crack Sealant Bending Beam Rheometer (CSBBR)

BBR Equipment Evaluation

Using the testing procedures summarized in Appendix A, the perceived softest and the stiffest sealants from one manufacturer were tested, along with an intermediate soft sealant from another manufacturer—BB, QQ and NN, respectively. The asphalt beam is supported at both ends by stainless steel half-rounds that are 102mm apart. The specimen, the supports, and the lower part of the test frame are submerged in a constant-temperature fluid bath, which controls the test temperature. During the test, the deflection of the center point of the beam is measured continuously. Sealants BB and NN were tested at -40°C, while sealant QQ was tested at -10°C.

Figure 9 shows time dependency for the load and deflection for sealant QQ. The maximum deflection was 0.7mm after 240s. Figure 10 shows the stiffness calculated using Equation (2) for four replicates of sealant QQ. At 60s, the average stiffness was 154MPa, with a standard deviation of 30.5MPa, and a coefficient of variation (COV) of 19.8%.

For sealant NN that was tested at -40°C, the maximum deflection limit of 6.3mm was reached after 62s of loading (Figure 11). An alternative test was performed with 50% reduction of the applied load. This reduction led to a smaller deflection; but the deflection still remained near the equipment limit (6mm) after 240s. The load was further reduced to 250mN, and a reasonable deflection of approximately 3mm was obtained. With the load of 250mN, the average stiffness after 60s was 12.7±0.60MPa, and the COV was only 4.6%.

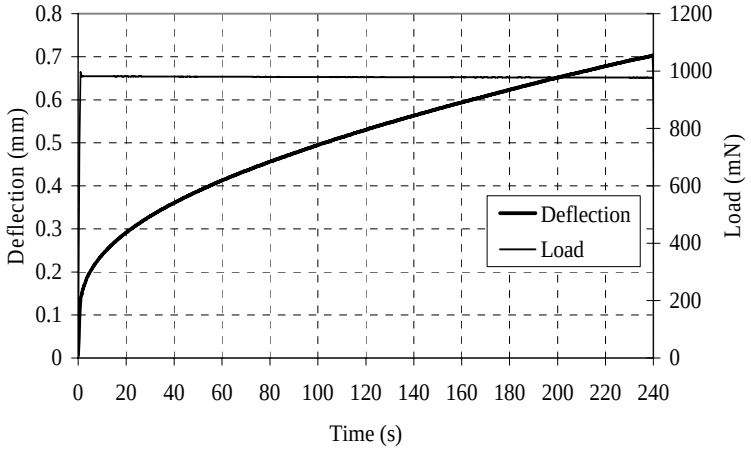

Figure 9. Load and Deformation versus Time for Sealant QQ Using the Standard Binder Beam Dimensions at -10°C

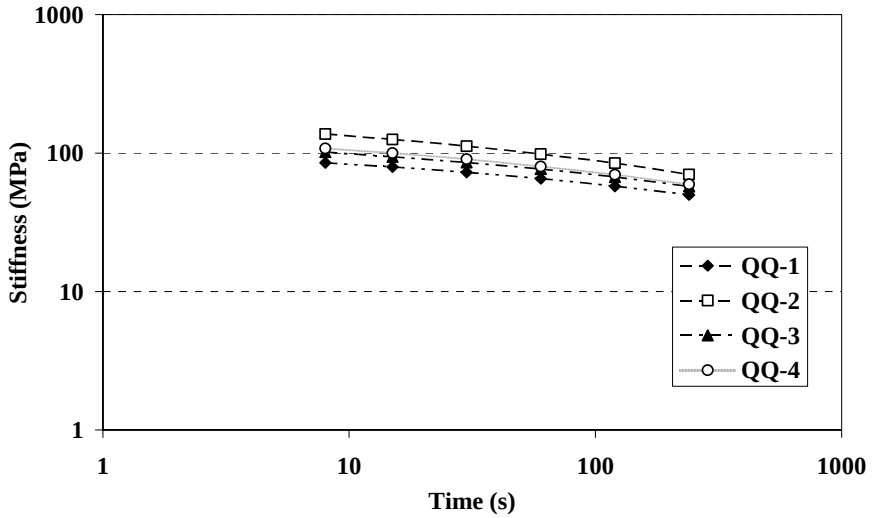

Figure 10. Stiffness versus Time for Sealant QQ Using the Standard Binder Beam Dimensions at -10°C

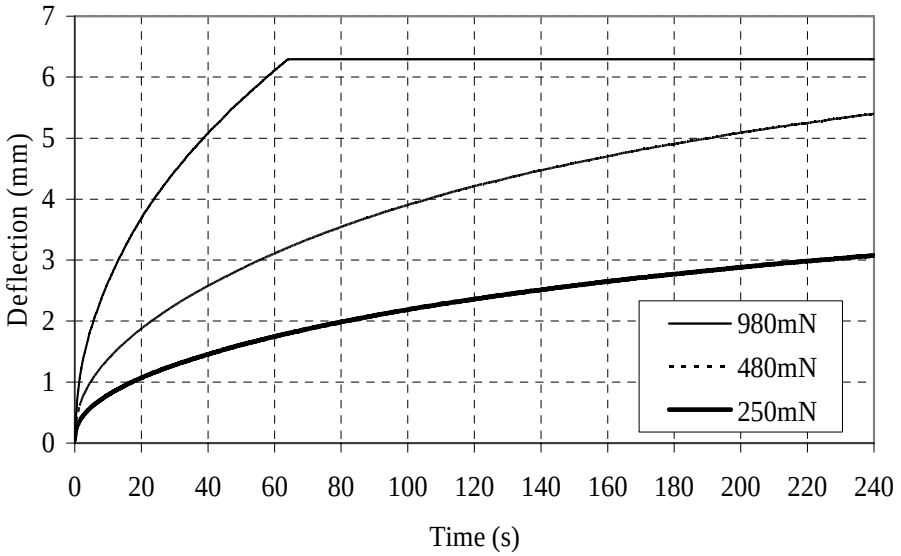

Figure 11. Deflection versus Time for Sealant NN for Three Loadings Using the Standard Binder Beam Dimensions at -40°C

For sealant BB, the deflection limit was reached after only 2s of loading at -40°C (Figure 12). With a load of 250mN, the deflection limit was reached after approximately 40s. When the load was reduced further to 100mN, the deflection was 4.8mm. After 60s, the stiffness was 2.2MPa and the COV was 9.8%. With the 100mN load, however, the deflection was unstable.

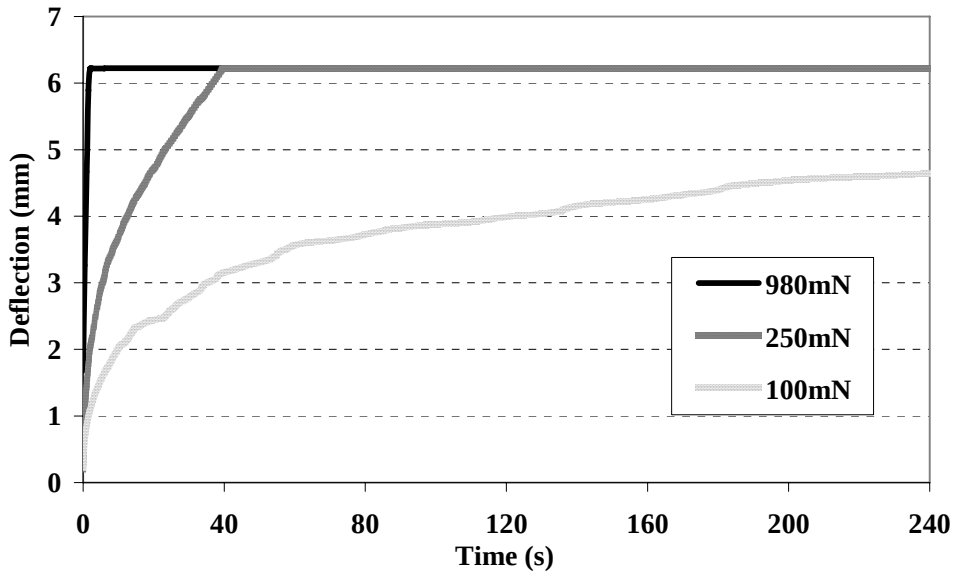

Figure 12. Deflection versus Time for Sealant BB for Three Loading Magnitudes Using the Standard Binder Beam Dimensions at -40°C

Modifications to the Asphalt Binder Test Procedure

Release Agent for Crack Sealants

To examine the effect of silicone grease material on the BBR results, testing with PG64-22 binder was performed on nine specimens using Mylar strips and on nine specimens using silicone grease. Table 3 shows the results of a t-test analysis (two samples assuming equal variances) conducted on the calculated stiffness values. The results show that the p-values are greater than the 0.05 level of significance. This indicates that there is no evidence of significant difference in the means. Therefore, statistically, the results obtained using the Mylar strips are equivalent to those using the silicone grease. Since silicone grease was proven not to affect the BBR results and was effective in preventing crack sealants from adhering to the aluminum molds, it was used in all the crack sealant testing conducted in this study, and will be recommended in the final test specification procedure presented at the end of this report.

Specimen Dimensions

The beam thickness was doubled from 6.35 to 12.7mm, to overcome the aforementioned problems resulting from the fact that crack sealant materials may exhibit very large deformations during the BBR test. A specimen mold was constructed for this purpose. Figure 13 shows the new mold and the schematic of new beam dimension of crack sealant.

Table 3. Statistical Analysis for the Stiffness (MPa) of Crack Sealants Using Two Release Agents

	Mylar Strip	Silicone Grease
Mean	68.13	67.07
Variance	2.83	4.63
Observations	9	9
Pooled Variance	3.73	
Hypothesized Mean Difference	0	
Df	16	
t Stat	1.17	
p(T<=t) one-tail	0.132	
t Critical one-tail	1.742	
p(T<=t) two-tail	0.262	
t Critical two-tail	2.12	

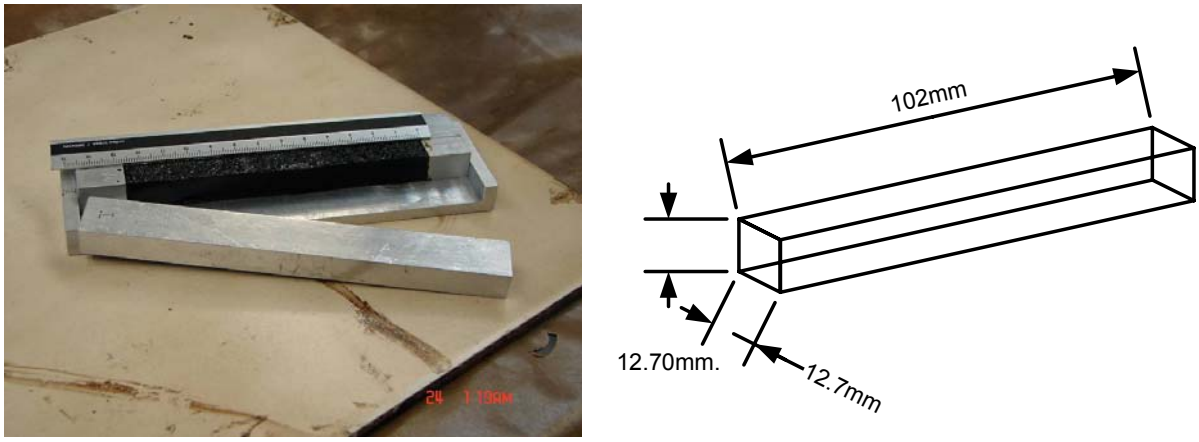

(a) (b)

Figure 13. (a) Newly Designed BBR Mold and Crack Sealant Beam; (b) Schematic of New Beam Dimension

Three replicates of sealant BB were tested using the new beam dimensions. Figure 14 shows the deflection versus time as well as the load versus time for one of the tested specimens. The load and deflection were stable over time. The maximum measured deflection was approximately 3.2mm and the measured stiffness was 6.1MPa, with a COV of 3.5%, after 60s of loading. The above results suggest that a 12.7mm-thick beam for testing hot-poured bituminous-based crack sealant materials was feasible. However, because of the increase in the beam's thickness, the deflection due to shear would increase. An analysis to determine the percentage of the deflection due to shear is presented in Appendix B. This analysis shows that center deflection contributed by shear force is only 4%, which was deemed acceptable (Al-Qadi et al., 2005).

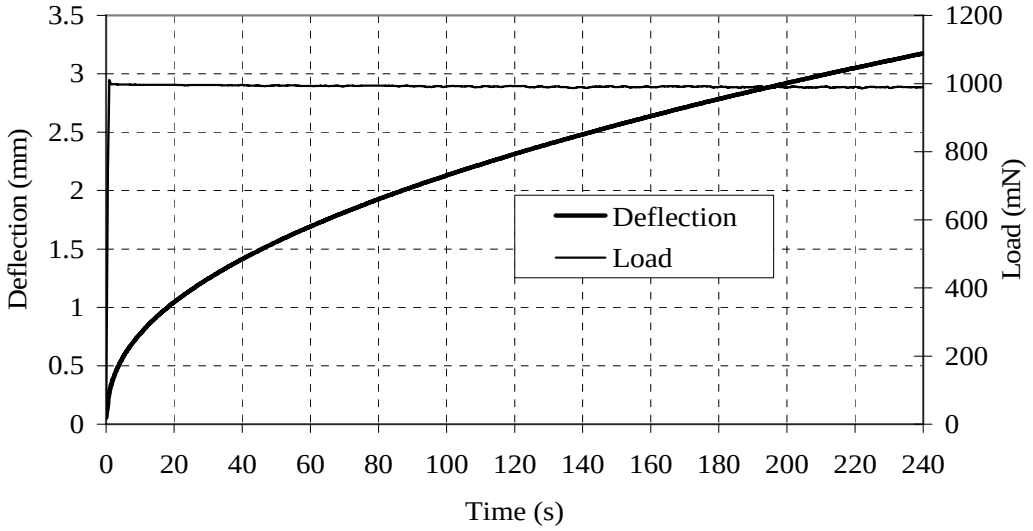

Figure 14. Deflection and Load versus Time for Sealant BB Using the New Beam Thickness of 12.7mm at -40°C

Test Repeatability

The repeatability of testing using the new beam size in CSBBR was studied by testing ten various sealants at -40°C (Sealants BB, CC, GG, HH, LL, MM, NN, PP, SS, and WW) and three sealants (Sealants MM, NN, and PP) at -35°C, -30°C, -28°C, -25°C, and -20°C. In addition, three sealants, described as hard (Sealants QQ, YY, and ZZ), were tested at -10°C. A minimum of three replicates per sealant were tested. Figure 15 shows the measured stiffness after 60s of loading (S_{60}) for the 10 tested sealants at -40°C. Figure 16 shows the measured S60 for sealants MM, NN, and PP versus temperature, while Figure 17 shows the measured S_{60} for the three sealants tested at -10°C. The highest calculated COV for all tested sealants was found to be 17.1%, while the minimum COV was 1.5%. Figure 18 shows the frequency distribution and the cumulative frequency distribution for the calculated COV. From this figure, it is noted that the most frequent calculated COV was between 6% and 8% (28.6% of the measurements). All measurements had a COV of less than 19%; almost 11% of the measurements had a COV of less than 4%, and almost 72% of the measurements had a COV of less than 10%.

To verify the acceptance of the range of the different results, limits as specified per ASTM C670-03 (Standard Practice for Preparing Precision and Bias Statements for Test Methods for Construction Materials) were checked. All calculated ranges were below the ASTM specified criteria of 3.3 standard deviations when testing three replicates and 3.6 standard deviations when testing four replicates.

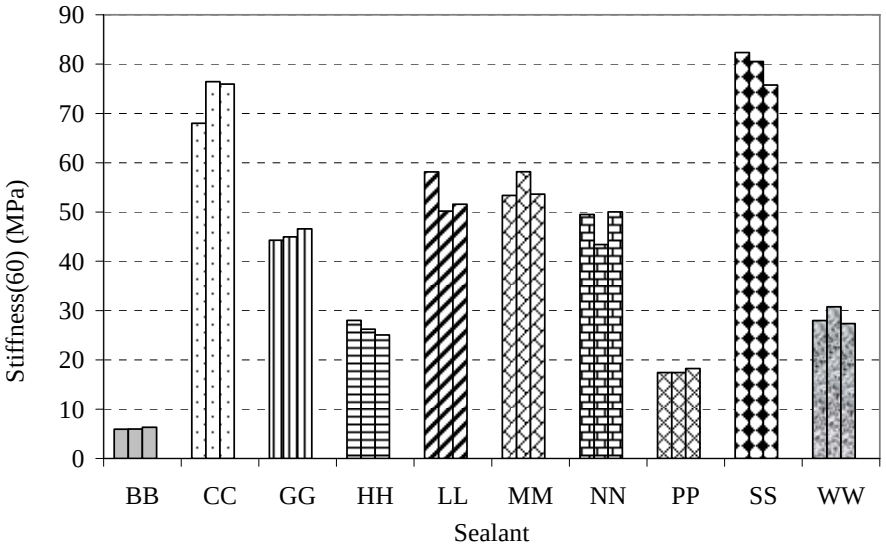

Figure 15. Measured Stiffness at 60s for Ten Sealants at -40°C

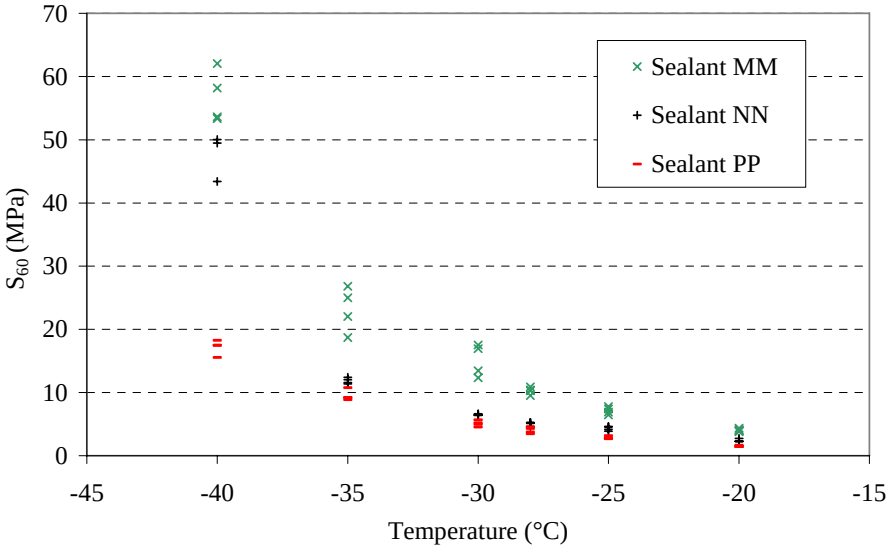

Figure 16. Measured Stiffness at 60s versus Temperature for Sealant MM, NN, and PP

To evaluate whether the testing shows differences between sealants tested at the same temperature, a Fairwise comparison with Tukey adjustments was performed on the measured S60 for the ten sealants tested at -40°C. This type of analysis must have homogeneity between the variances. To check this hypothesis for the data, the residuals versus the predicted S60 was plotted, as shown in Figure 19a. A trend is noted: namely, that as S60 increases so does the residual. This finding suggests that a transformation of S60 is needed to compare the results. A natural logarithm transformation was applied to S60 and was plotted against the residuals, as shown in Figure 19b. No trend was found to exist between the natural logarithm of S60 and the residuals. Hence, a Fairwise comparison with Tukey adjustments could be performed on the transformed data. Table 4 shows the results of the analysis. The numbers indicate the group of products that are statistically similar. Sealants SS and CC are statistically similar; Sealants MM, LL, and NN are statistically similar; Sealants NN and GG are statistically similar; Sealants WW and HH are

statistically similar; and Sealants PP and BB are statistically different from all other sealants as well as from each other.

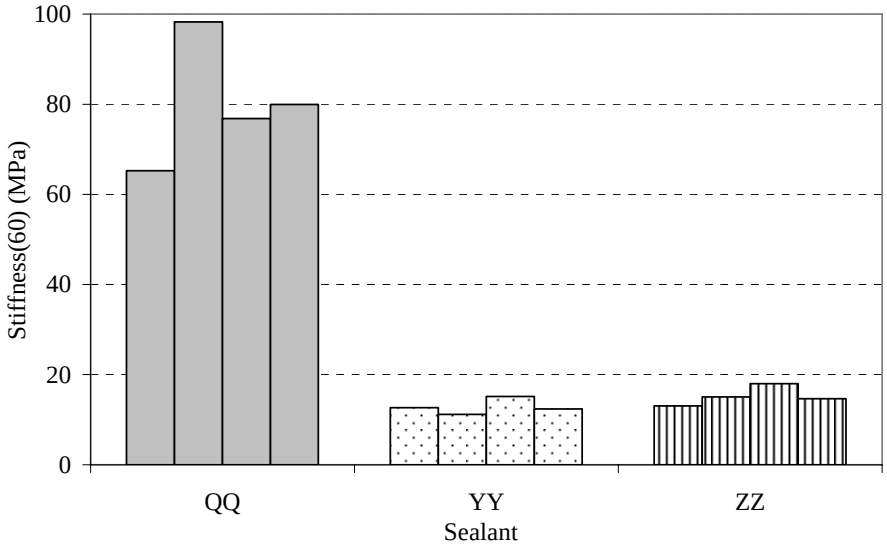

Figure 17. Measured Stiffness at 60s for Three Sealants at -10°C

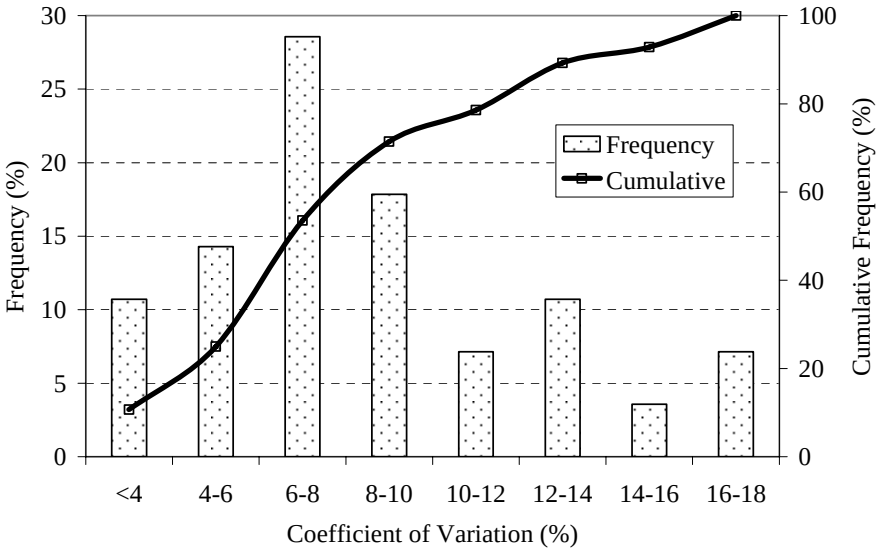

Figure 18. Frequency Distribution of the COV

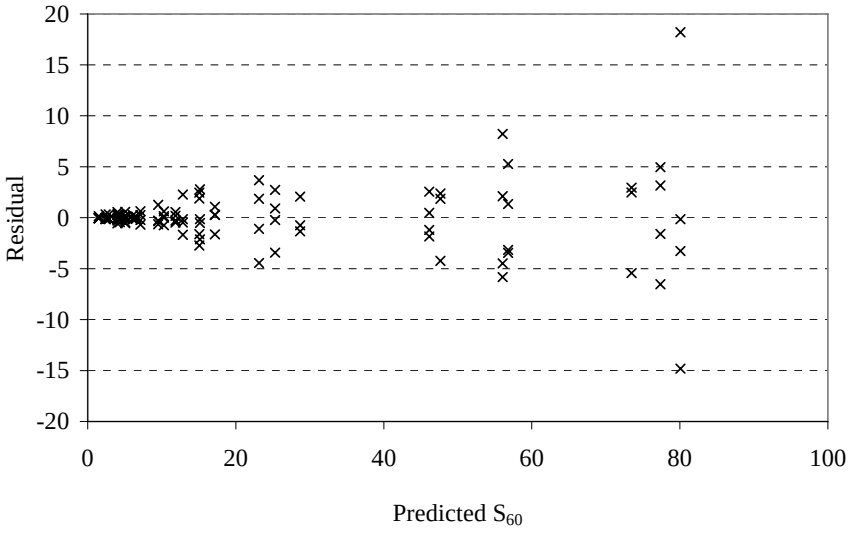

(a)

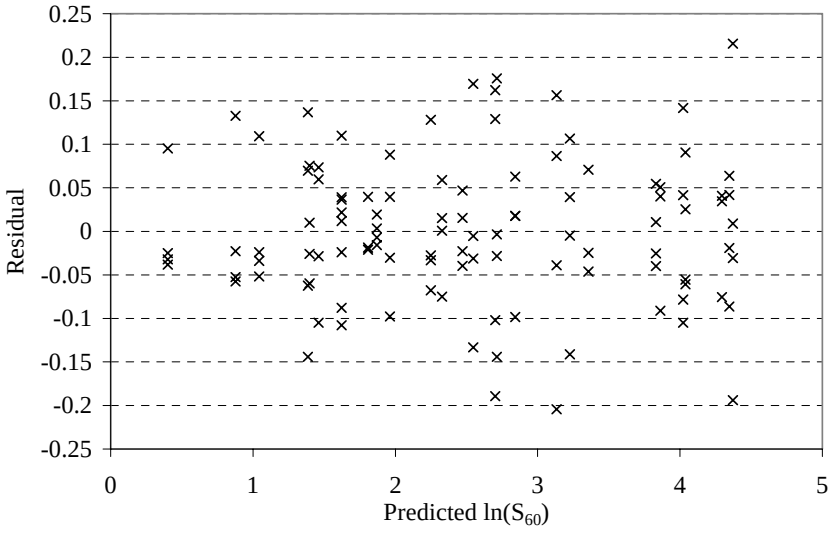

(b)

Figure 19. (a) Residuals versus Predicted S_{60}, (b) Residuals versus Predicted ln (S_{60})

Table 4. Results of the Fairwise Comparison with Tukey Adjustments on ln(S_{60})

Sealant	Mean					
SS	4.3466	1				
CC	4.295	1				
MM	4.038		2			
LL	4.0217		2	3		
NN	3.8615		2	3	4	
GG	3.8307				4	
WW	3.3568					5
HH	3.2268					5
PP	2.843					
BB	1.808					

Sealant MM, NN, and PP were further evaluated to investigate the effect of temperature on their measured S_{60}. As shown in Figure 20, plotting $\ln S_{60}$ versus temperature results in a linear relationship for all three sealants. Therefore, one may assume that S_{60} varies exponentially with temperature in this temperature range for all three sealants as follows:

$$\ln S_{60} = a + bT \quad (16)$$

where,

$\ln S_{60}$ = natural logarithm of the measured stiffness after 60s of loading;
T = test temperature in °C; and
a and b = regression parameters.

The statistical package SAS was used to determine the regression parameters for the three sealants that fit Equation (16). Table 5 presents the results of this regression analysis.

Table 5. Regression Parameters for Sealants M, N, and P

Parameter	Estimate	Std Error	Approximate 95% Confidence Limits	
a_MM	-1.8267	0.2032	-2.2325	-1.4208
b_MM	-0.1462	0.00529	-0.1568	-0.1356
a_NN	-5.2556	0.4877	-6.2295	-4.2816
b_NN	-0.2276	0.0124	-0.2524	-0.2028
a_PP	-1.9727	0.5101	-2.9916	-0.9539
b_PP	-0.1205	0.0135	-0.1475	-0.0935

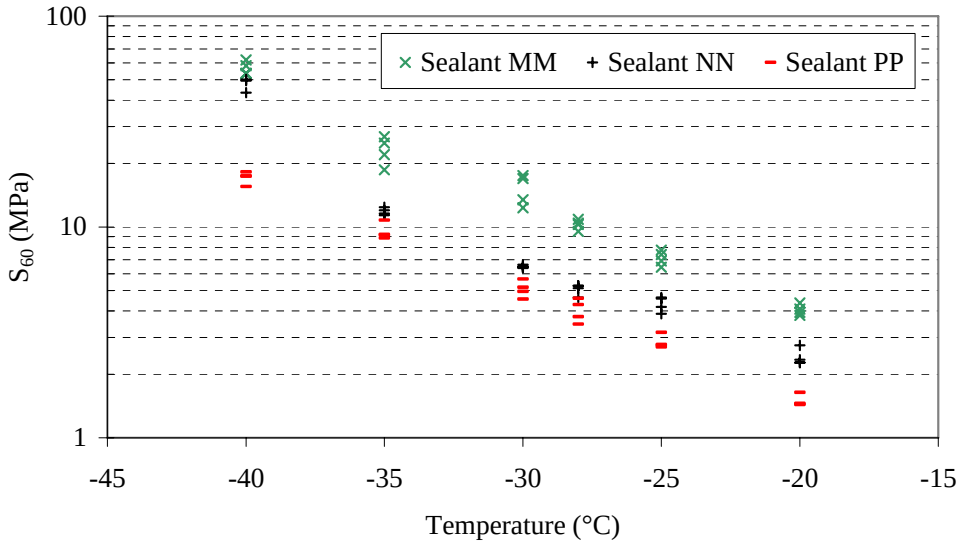

Figure 20. S_{60} versus Temperature for Sealants MM, NN, and PP

Time-Temperature Superposition Principle Verification at Low Temperature

To verify the linear viscoelastic assumption, the first condition was verified by apply three levels of loading (250mN, 490mN, and 980mN) on the sealant specimen. Test results indicated that stiffness was independent of the applied stress level, as shown in Figure 21. This finding was verified by Al-Qadi et al. (2006), who concluded that stiffness independent of the load level is applicable for sealants at low temperature.

The second condition of linearity, however, could not be verified experimentally due to the sealant's softening behavior, which results in the material creeping due to the seating load (35mN). Testing the soft sealant BB at -34°C indicated that as the creep load (980mN) is removed, the material recovers some of the exhibited deformation but then creeps after 50s of unloading (Figure 22). Therefore, an analytical approach to investigate the second condition of linearity using the finite element (FE) method was conducted. The recovery curve was obtained by subtracting the experimental data from the extrapolated values at a time period between 240 and 480s (Figure 23). For a linear viscoelastic material, the experimental deflection at time (t) and the recovery deflection at time 240s + (t) should be equal, or within 5% deference (Marasteanu and Anderson, 2000). Table 5 summarizes the measured deflections for sealants AB, NN, YY, and ZZ at 120 and 240s and the corresponding FE measurements at 360 and 480s, respectively. It was found that by using two points in the deflection curves, the maximum difference was less than 4%. This analysis indicates that the second condition of linearity has been validated.

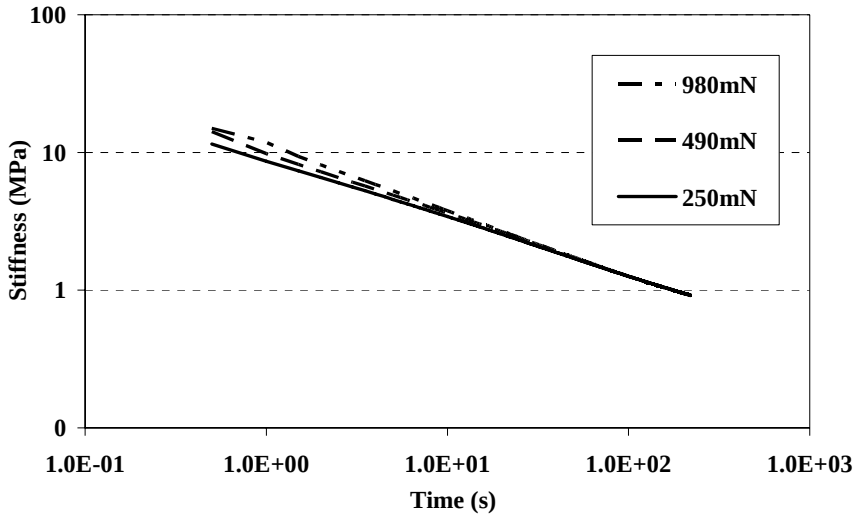

Figure 21. Measurements of Creep Stiffness for Sealant NN at -40 °C

Table 6. Analytical Results to Verify the Time-Temperature Superposition Principle

Sealant	Exp. def. at 120s (mm)	FE def. at 360s (mm)	Error (%)	Exp. deflection at 240 sec (mm)	FE def. at 480s (mm)	Error (%)
AB	1.60	1.63	1.55	2.04	2.03	0.66
NN	1.12	1.09	3.47	1.49	1.44	3.84
YY	0.48	0.48	0.14	0.62	0.63	0.92
ZZ	1.75	1.74	0.50	2.32	2.25	2.80

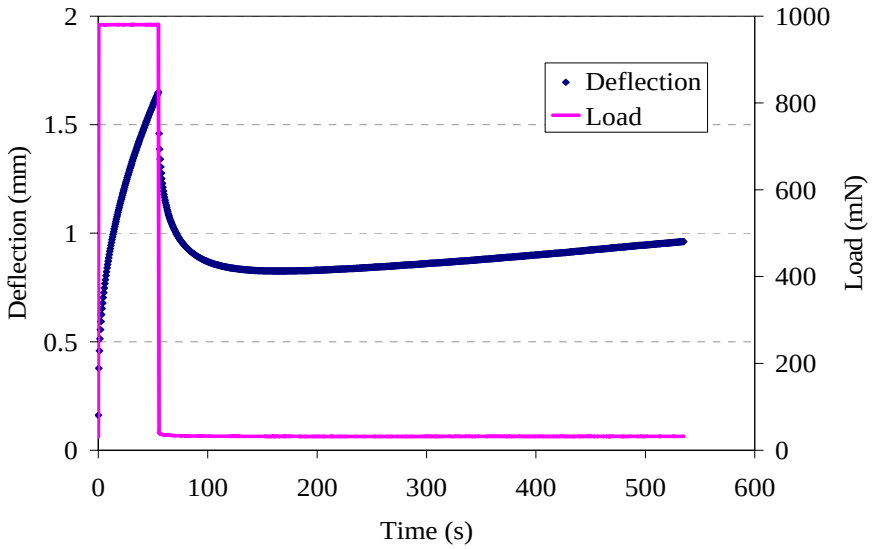

Figure 22. Creep Measurements for Sealant BB at -34 °C

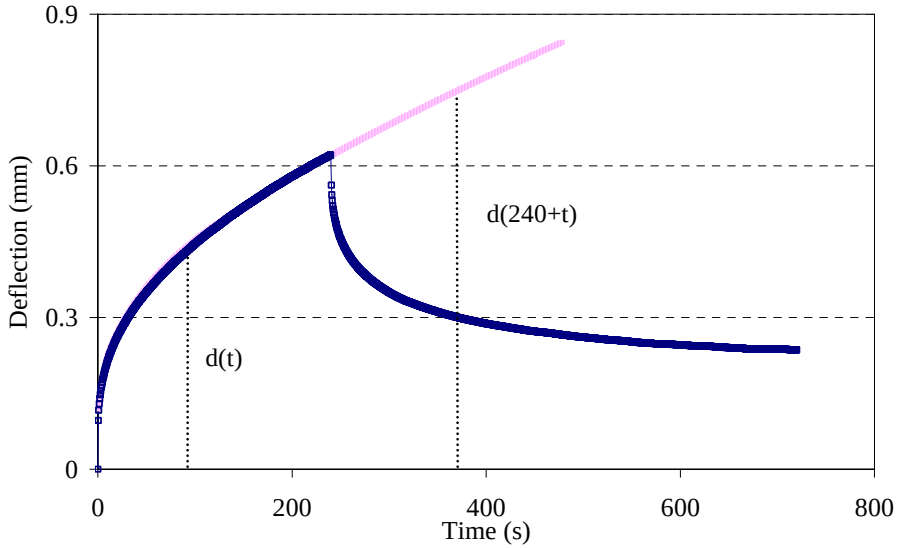

Figure 23. Schematic Diagram Illustrates the Extrapolated Data after 240s, Using FE

Effect of Aging

A comparison of sealant aged in the laboratory following the proposed procedure is presented in Figure 24. Twelve sealants were selected to present the effect of aging after the vacuum oven aging procedure had been performed. Sealant BB, VV, and AB show little or no softening after the vacuum aging. Sealant WW, QQ, PP, MM, NN, YY, ZZ and UU show stiffening after the vacuum oven aging. The results show that the level of sealant softening or stiffening after the vacuum oven aging is varied and it mainly dependent on the chemical composition of the sealant according to the study by Masson et al. (2003).

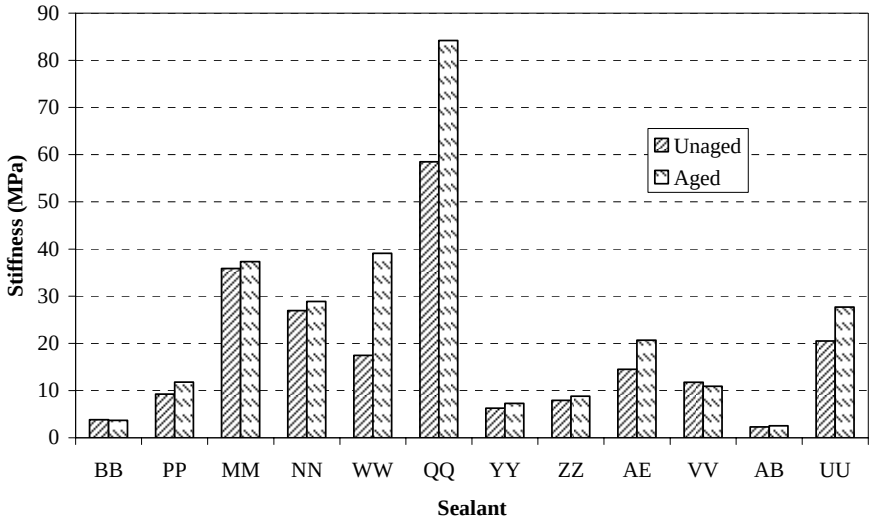

Figure 24. Effects of Aging on Twelve Selected Sealants

Cohesive Performance at Low Temperature – Laboratory Parameters

Crack Sealants Stiffness (S)

Table 7 presents the stiffness measurements for 15 sealants considered in this study. Repeatability of the measurements is also presented in this table for three replicates of aged sealants. The stiffness of sealants BB, PP, AD, NN, WW, MM, and DD was measured at -40°C, -34°C, and -28°C; AE was measured at -34°C, -28°C, and -22°C; UU and VV were measured at -22°C, -16°C, and -10°C, and sealants AB, YY, ZZ, EE, and QQ were measured at -16°C, -10°C, and -4°C. The lowest stiffness measured at -40°C, sealant BB, was 3.15MPa with COV of 4.35%. The stiffness threshold was determined to be 25MPa based on the correlation with the results of the limited samples installed in Montreal in early 1990s. Details of the validation analysis are presented under Field Validation section.

Average Creep Rate

Table 7 shows the average creep rate for the tested sealants. The data show that generally, the average creep rate increased with the increase in temperature. The average creep rate threshold was determined to be 0.31 based on the correlation with the results from the limited samples installed in Montreal in early 1990s..

Dissipated Energy Ratio

Table 7 presents the average values of dissipated energy ratios for tested sealants. It is preferable to have a higher energy dissipation ratio. If the ratio is greater than unit, it implies the material has the ability to dissipate the imposed loading more quickly. A higher ratio number is useful when selecting crack sealant materials because an important property

of the material is the ability to relax the imposed load. For simplicity, the dissipated energy ratio threshold will not be included in the performance-based guideline.

Table 7. CSBBR Test Results for Aged Sealants under Varying Temperatures

Sealant	Temp (°C)	S_{240} (MPa)					Avg Creep Rate	Dissipated Energy Ratio	
		Rep. 1	Rep. 2	Rep. 3	Avg	COV (%)		Ratio	Error (%)
QQ	+2	12	12	13	12	2.9	0.49	0.9	3.3
	–4	34	35	32	34	3.2	0.38	0.6	2.9
	–10	84	87	86	86	1.5	0.26	0.7	3.4
EE	–4	5	5	4	4	4.0	0.45	1.8	2.1
	–10	8	9	9	9	4.2	0.37	0.7	5.3
	–16	23	23	27	24	8.5	0.31	0.3	9.5
ZZ	–4	3	3	3	3	8.9	0.46	2.4	3.7
	–10	8	9	9	9	7.5	0.43	0.9	3.6
	–16	27	26	25	26	2.9	0.37	0.4	3.5
YY	–4	3	3	3	3	5.0	0.44	2.5	4.1
	–10	7	8	8	7	5.6	0.41	1.0	4.4
	–16	18	18	18	18	0.9	0.34	0.4	7.5
AB	–4	3	2	3	3	3.9	0.37	2.2	4.0
	–10	6	6	6	6	1.9	0.35	1.1	3.8
	–16	12	11	11	12	1.4	0.30	0.5	4.1
VV	–10	4	4	4	4	0.4	0.46	2.1	4.1
	–16	11	10	11	11	3.6	0.40	0.7	4.1
	–22	31	30	30	30	2.8	0.37	0.4	3.5
UU	–10	4	4	5	4	12.3	0.48	2.0	3.6
	–16	9	11	10	10	8.3	0.37	0.7	3.2
	–22	29	27	28	28	4.2	0.33	0.3	3.6
AE	–22	7	7	8	7	8.4	0.32	0.8	3.5
	–28	9	11	10	10	9.3	0.32	0.5	4.0
	–34	21	20	22	21	4.3	0.30	0.3	3.7
DD	–28	14	14	12	13	9.4	0.34	0.5	4.0
	–34	24	23	25	24	3.7	0.29	0.3	3.5
	–40	47	44	42	45	6.0	0.28	0.3	3.0
MM	–28	7	7	7	7	4.8	0.36	0.9	4.0
	–34	17	18	15	17	7.3	0.33	0.4	3.5
	–40	37	37	38	37	0.9	0.33	0.4	3.2
WW	–28	6	6	6	6	6.6	0.42	1.1	4.2
	–34	14	17	14	15	9.6	0.43	0.6	3.7
	–40	42	36	40	39	7.7	0.39	0.5	3.4
NN	–28	6	6	6	6	4.0	0.35	0.9	4.5
	–34	11	12	11	12	1.0	0.34	0.6	4.3
	–40	28	29	28	28	2.7	0.34	0.3	3.7
AD	–28	4	4	4	4	6.6	0.36	1.3	4.6
	–34	11	11	10	11	6.1	0.33	0.5	3.6
	–40	24	21	24	23	8.1	0.31	0.3	4.1
PP	–28	Exceeded Machine Limit							
	–34	3	3	3	3	6.1	0.45	2.2	4.0

	–40	11	12	12	12	7.6	0.41	0.6	3.5
BB	–28	Exceeded Machine Limit							
	–34								
	–40	3	3	3	3	4.4	0.43	2.1	4.5

Viscoelastic Behavior and Modeling

Data Reduction and Analysis

It is usually a delicate process to effectively fit a Prony-series expansion to creep measurements. The fitting process is highly sensitive to data scattering and it is not unusual to obtain negative unrealistic coefficients. Different methods were presented to adequately fit the Prony-series to experimental data with various degrees of success (Park and Kim 2001). Given the limited time-spectrum of the experiment, the fitting process of the CSBBR data was relatively easy. However, it was particularly important to ensure that the trend of the parameters was realistic with respect to the change in temperature. Therefore, using the developed procedure, described in this section, is strongly recommended.

For a total loading of 240s, using the logarithm of the loading time (log t), as recommended by ABAQUS (2005), three Prony-series terms were needed to obtain an acceptable fit of the measured creep response. The curve fitting is started by specifying the Poisson's ratio, the number of Prony series terms, the initial stiffness magnitude, and other constraints under long-term loading. It was assumed that the response of the beam at time 0.5s is associated with the initial elastic response of the material. Therefore, the initial creep compliance (D_0) was determined directly from the measured compliance after initial loading. The fitting process for the other parameters was then conducted using a nonlinear statistical package; it can be easily performed using the optimization technique available in most spreadsheet solvers.

From the results presented in Table 8, the change in the relaxation modulus coefficient (E_i) is in agreement with the change in temperature. It is expected that as the temperature decreases, the material becomes more brittle, and therefore, the modulus component (i.e., spring) of each element should increase; each Kelvin element is associated with the response of a given material component. It may also be noticed that the modulus of the individual spring was always greater than the modulus associated in each Kelvin element (e.g. $\xi_1 > \xi_2 > \xi_3$).

To account for the sensitivity of data scattering – which may result in unrealistic coefficients and multiple solutions – the fitting process was constrained by the following condition to obtain a unique solution for each sealant:

$$\xi(\infty) = \frac{D_0}{D(\infty)} = 1 - \sum_{i=1}^{K} \zeta_i \qquad (17)$$

To determine $\xi(\infty)$, creep compliances measured at 240s were compared to those measured over an extended loading time of 7200s. Results, presented in Figure 25, indicated that the calculated creep after 240s is considered indicative of longer loading times. Therefore, $D(\infty)$ was determined to be 150% of the measured creep at 240s. Figure 26

and Figure 27 show that the fitting would result in a model capable of describing the material's response to creep loading.

Although the aforementioned analysis verified that the Prony series model may be used to describe the constitutive behavior of crack sealants, the acceptable fitting of the measurements does not ensure that the adopted model is suitable to describe the material's creep response to loading. Because a closed-form solution cannot be easily incorporated into the analysis of a crack sealant, the mechanical analysis of this problem may only be achieved using numerical methods such as FE. Therefore, FE analysis was performed to compare the model's response to creep loading and the measured deflections by CSBBR at different temperatures. Through this process, the applicability of the linear viscoelastic theory was verified.

Table 8. Summary of Fitted Prony Series Parameters for Sealants at Low Temperatures

Sealant	Temp (°C)	E_o	ξ_1	ρ_1	ξ_2	ρ_2	ξ_3	ρ_3
AB	-10	49.1	5.8E-01	1.6E+00	2.1E-01	23.4	1.6E-01	287.4
	-4	35.6	5.9E-01	1.6E+00	2.1E-01	22.6	1.5E-01	273.1
BB	-40	71.8	7.5E-01	1.3E+00	1.5E-01	17.6	7.6E-02	160.8
	-34	33.8	7.2E-01	1.4E+00	1.8E-01	18.6	8.9E-02	236.8
DD	-40	151.2	4.8E-01	2.5E+00	4.8E-01	42.5	1.2E-02	148.8
	-34	88.8	6.1E-01	1.9E+00	1.8E-01	25.6	1.7E-01	70.9
MM	-40	271.9	6.0E-01	1.8E+00	2.1E-01	19.8	1.4E-01	217.8
	-34	171.3	6.6E-01	1.6E+00	1.9E-01	19.6	1.2E-01	227.5
	-28	35.1	6.7E-01	1.5E+00	2.0E-01	18.0	9.2E-02	71.0
NN	-40	193.1	6.9E-01	1.5E+00	1.8E-01	18.4	8.9E-02	201.2
	-34	85.2	7.2E-01	1.4E+00	1.6E-01	18.1	8.7E-02	181.4
	-28	35.8	7.1E-01	1.4E+00	2.3E-01	19.3	3.6E-02	173.6
PP	-40	230.5	7.9E-01	1.1E+00	1.4E-01	17.2	5.1E-02	171.3
	-34	87.0	7.6E-01	8.5E-01	1.6E-01	9.5	6.3E-02	74.7
QQ	-10	410.8	4.8E-01	2.3E+00	2.7E-01	22.9	2.1E-01	280.0
	-4	233.6	6.6E-01	1.7E+00	2.0E-01	15.9	1.1E-01	104.9
WW	-40	509.3	5.0E-01	2.5E+00	2.6E-01	23.6	1.9E-01	274.9
	-34	149.1	6.9E-01	7.1E-01	1.8E-01	10.0	1.0E-01	75.4
	-28	60.6	7.7E-01	1.3E+00	2.0E-01	20.3	1.3E-02	245.7
YY	-10	104.2	5.2E-01	2.1E+00	2.4E-01	21.8	1.9E-01	240.0
	-4	31.8	7.4E-01	1.4E+00	1.6E-01	15.1	7.3E-02	117.6
ZZ	-10	118.5	6.0E-01	1.1E+00	2.1E-01	13.3	1.3E-01	111.2
	-4	41.8	6.4E-01	1.4E+00	2.0E-01	20.2	1.2E-01	194.1

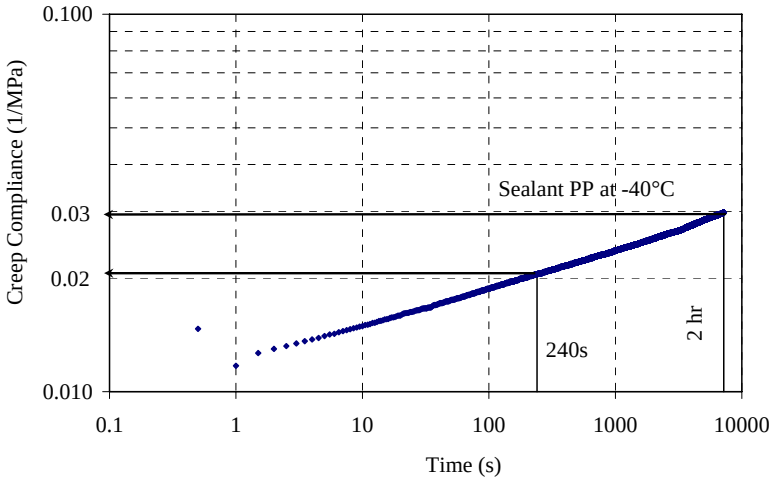

Figure 25. Comparison of Creep Compliance after 240s and 7200s of Loading

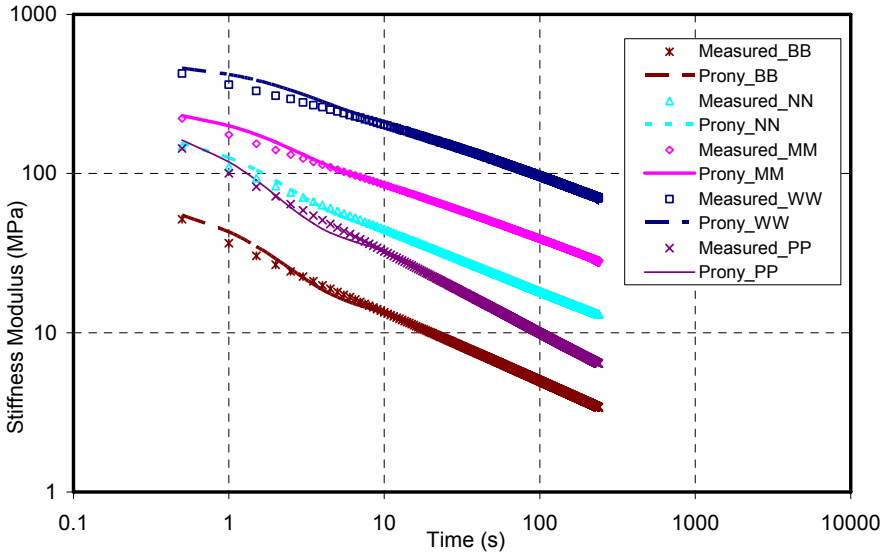

(a)

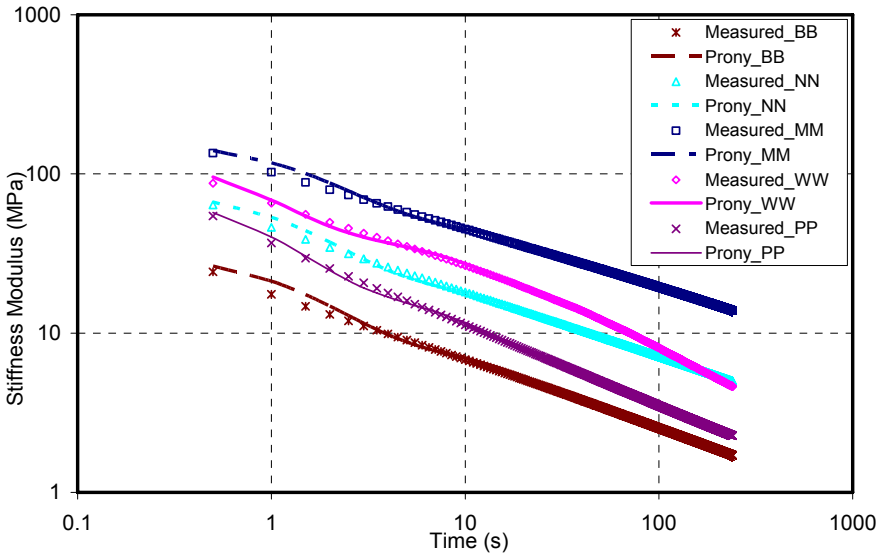

(b)

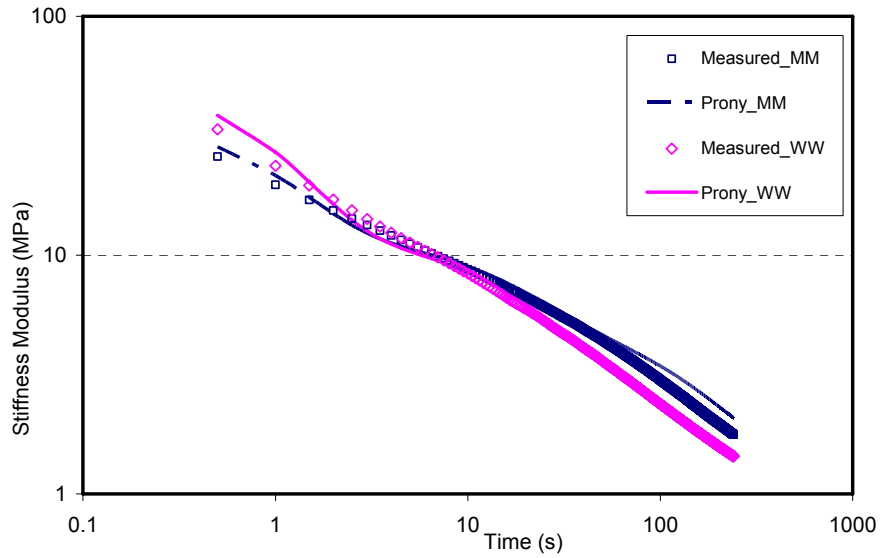

(c)

Figure 26. Measured and Predicted Stiffness Moduli over Time at a) -40; b) -34°C; and c) -28°C

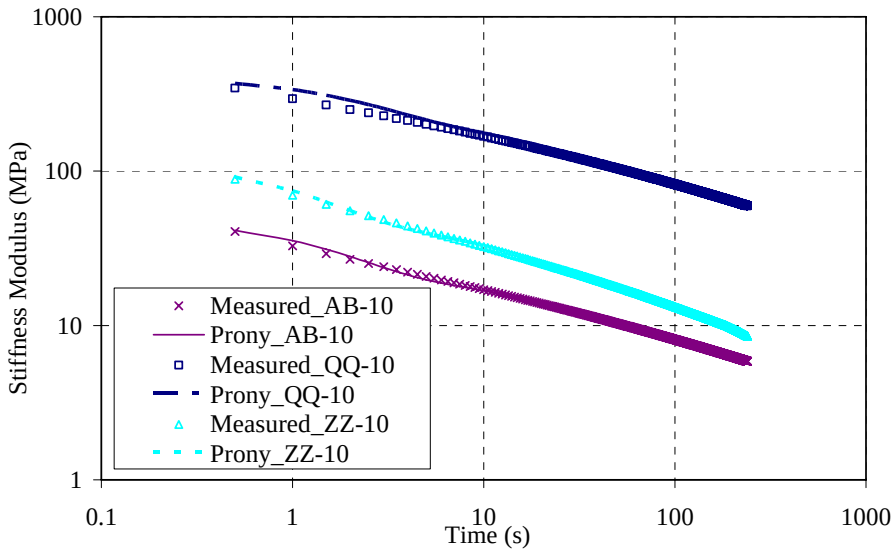

(a)

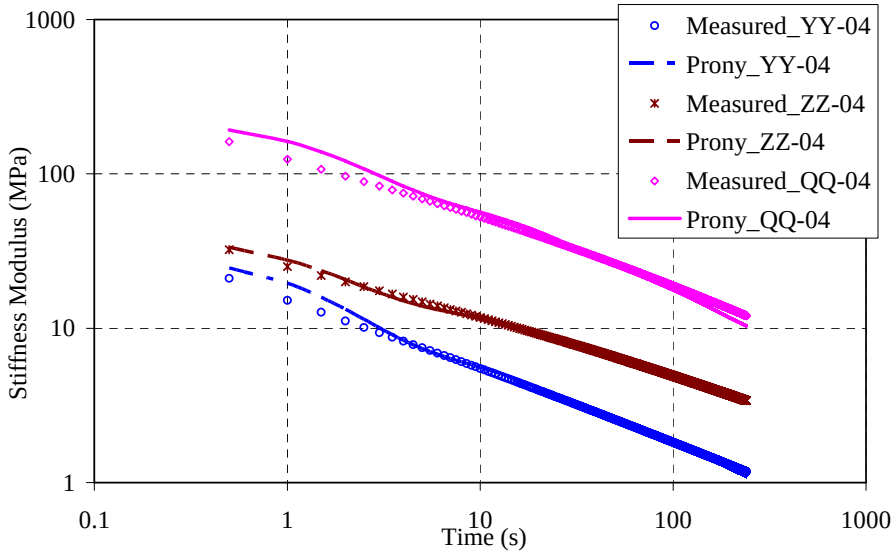

(b)

Figure 27. Measured and Predicted Stiffness Moduli over Time at a)-10°C; and b)-4°C

Model Validation

Figure 28 (a through e) show the deflection measurements during the loading and unloading process for 10 sealants. Each curve represents an average of three replicates. As would be expected, sealant response is affected by testing temperature; a larger deflection is associated with a higher temperature. The maximum deformation was recorded when sealant YY was tested at -4°C, while the minimum was obtained when sealant WW was tested at -40°C. The deflection at 720s did not fully recover due to the residual forces initiated from the weight of the sealant sample and most importantly, the setting load of 30mN, which is essential to maintain the contact of the loading nose to the beam during the unloading process. Considering the relatively soft nature of crack sealant, the result of those loads has a considerable effect on the overall unloading response.

As shown in Figure 28 (a through e), the FE model, as described by the Prony series parameters, closely matched the experimental data except for very soft sealants. Soft sealants exhibit excessive deflection; hence, the model under-predicted the recovery response of long-term unloading. This behavior can be attributed to one of two reasons. First, as time increases, the sealant becomes more viscous and the evolution of damage, in terms of microvoids, can contribute to higher deflection than what is predicted by the linear FE model; second, as temperature increases, it is possible that the material became more nonlinear viscoelastic. Soft sealants generally have a low glass transition temperature, indicating a viscoelastic behavior that deviates from the linear behavior, even at low service temperatures.

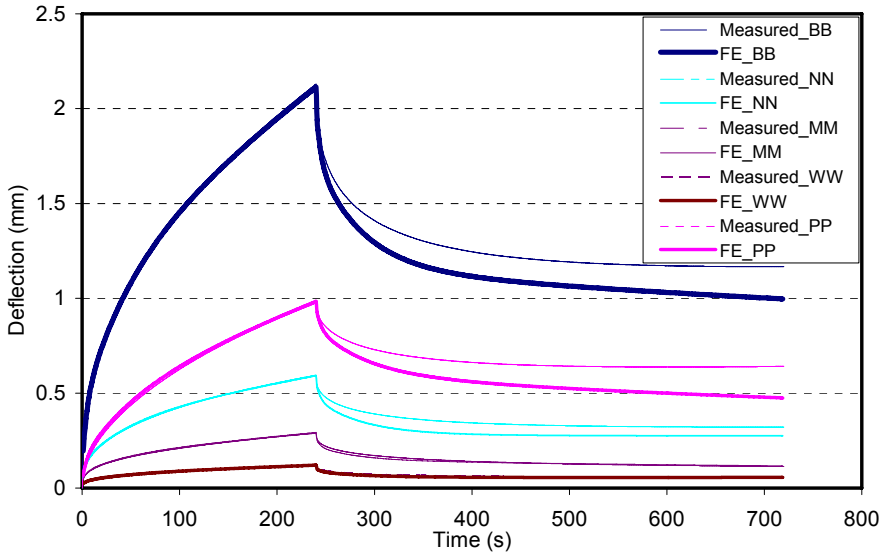

(a)

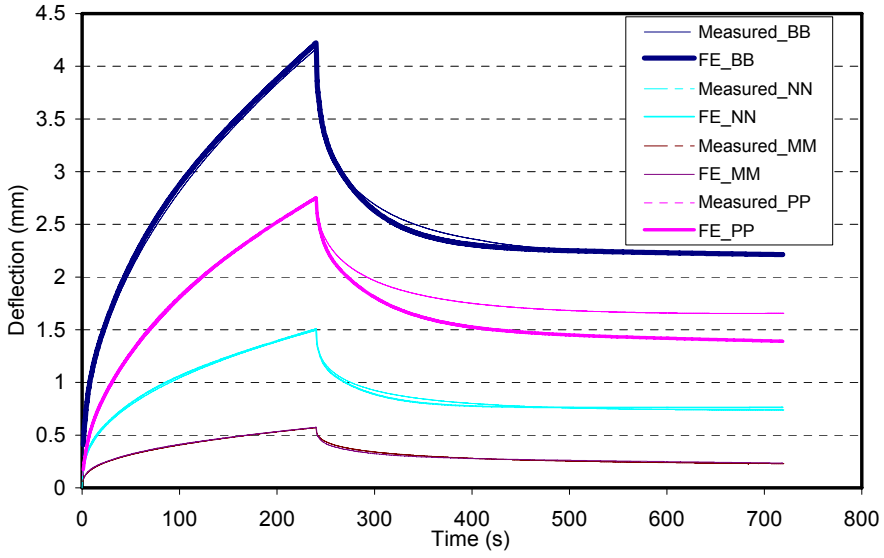

(b)

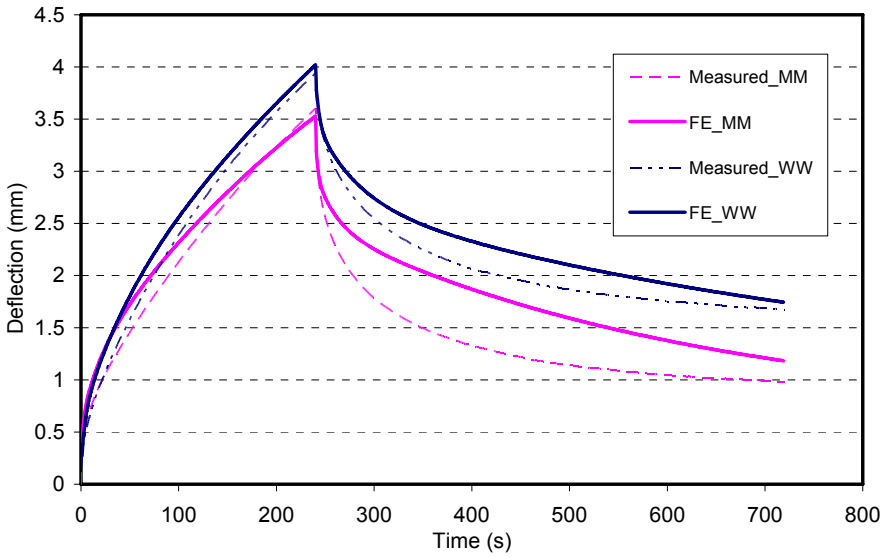
Measured_MM
FE_MM
Measured_WW
FE_WW
Deflection (mm)
Time (s)
0
0.5
1
1.5
2
2.5
3
3.5
4
4.5
0
100
200
300
400
500
600
700
800

(c)

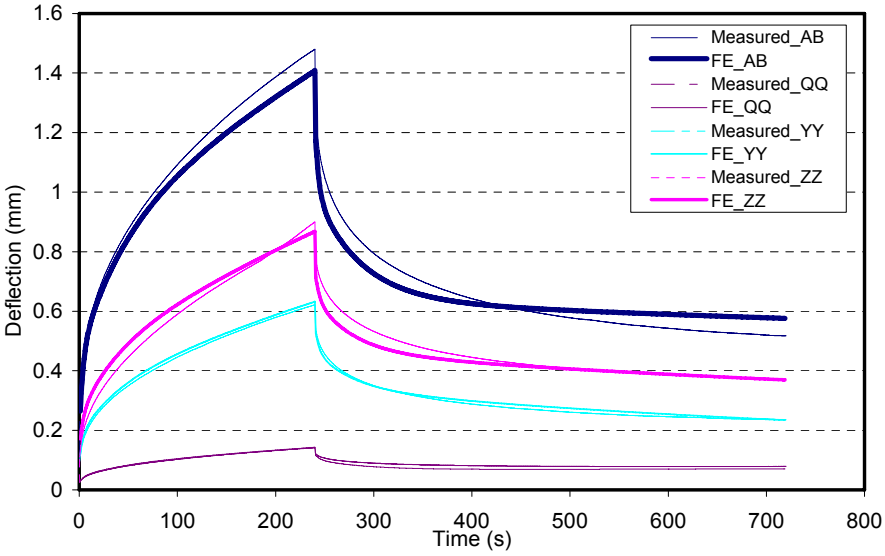
Measured_AB
FE_AB
Measured_QQ
FE_QQ
Measured_YY
FE_YY
Measured_ZZ
FE_ZZ
Deflection (mm)
Time (s)
0
0.2
0.4
0.6
0.8
1
1.2
1.4
1.6
0
100
200
300
400
500
600
700
800

(d)

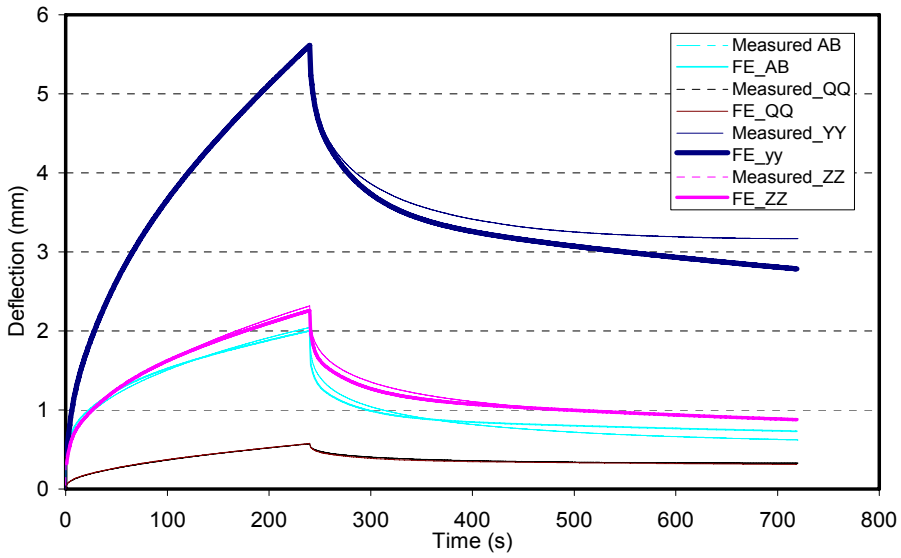

(e)

Figure 28. Relationship between Measured and Calculated Deflections at a) -40; b) -34; c) -28; d) -10; and e) -4°C

Test Variation

Precision and bias are two of the most important factors that must be considered when developing performance-based guidelines. Single-operator precision (repeatability) results, as defined in ASTM C670, were presented in Table 7. Precision is the measurement of the greatest difference between two or more test results that would be considered acceptable when properly conducted. Table 7 shows that repeatability of the stiffness measurements for all sealants conducted by a single operator is less than 10%. The results indicate that a good level of repeatability can be achieved if the test procedure developed in the study is followed.

For the variation study, two identified operators and two CSBBR devices by two manufacturers were utilized. Unaged sealants BB, WW MM, AE, VV and ZZ were selected for variation testing. They were selected because of the variation in their chemical composition and recommended various geographic location application. A statistical t-test, assuming that two samples have equal variance, was conducted to determine any significant differences among the selected operators and devices. As shown in Figure 29, at a 95% confidence level, no significant differences were detected for the stiffness values at 240s measured by the two operators using the same device. Results also revealed that one device recorded higher stiffness values than the other, as shown in Figure 30. The paired t-test results implied that there is a significant difference of the measured stiffness obtained from the two devices. To confirm this point, a standard material was further tested using the two devices.

The precision, stainless-steel, confidence beam supplied by a manufacturer was used to check the previous conclusion. Tests were conducted at four various temperatures (-40°C, -28°C, -16°C and -4°C) with eight tests performed at each temperature. A t-test assuming equal variance was conducted to examine if the results from the two devices are the same. As the results show in

Table 9, the means from devices I and II are 218GPa and 212GPa, respectively. Therefore, with 5% type I error, it is concluded that the population means from device I is different from device II. On further comparison of the results from the steel-beam and from the sealant material, an opposite trend was observed. The results from device I shows a lower value when sealant material was tested; but shows a higher value when the steel-beam was used. The reason might be attributed to the accuracy of the instrument itself in the different loading range, since the stiffness for the standard steel beam is very high (about 210GPa) and the stiffness for the crack sealant usually ranges from 10 to 30MPa, which is relatively low compared to the stainless steel beam. According to the aforementioned study, there appears to be a systematic difference between the two devices; an observation that was reported by others.

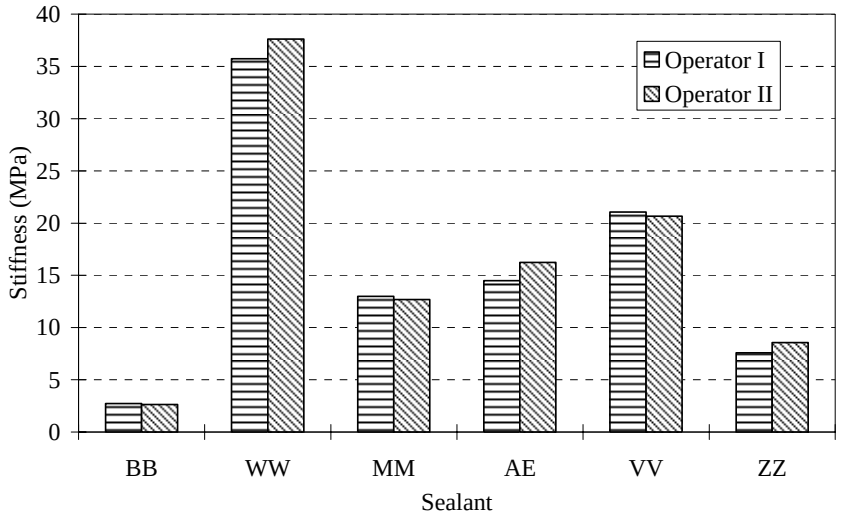

Figure 29. Comparison of Average Stiffness of Selected Sealants at 240s, between Two Operators

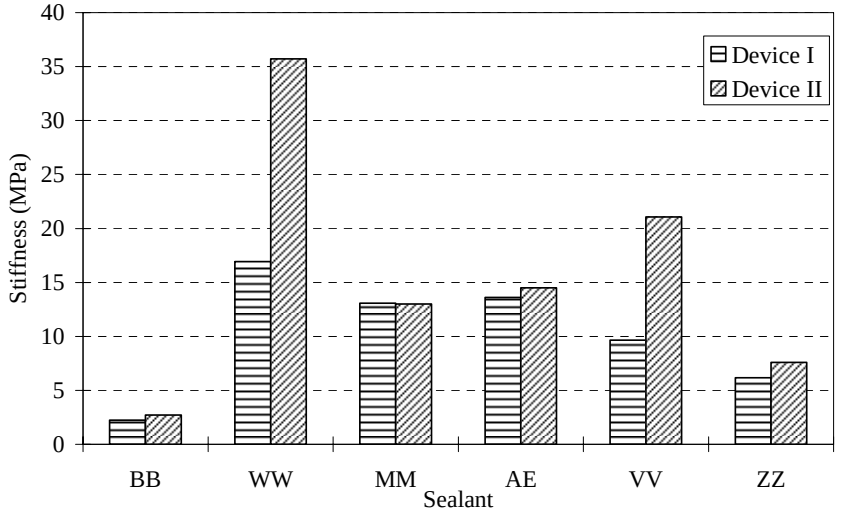

Figure 30. Comparison of Average Stiffness of Selected Sealants at 240s, between Two Devices

Table 9. Results of Steel Beam from Two-Sample t-test using Two Devices, Assuming Equal Variances

	Device I	**Device II**
Mean	218.00	212.19
Variance	21.23	39.64
Observations	32	32
Pooled Variance	30.44	
Hypothesized Mean Difference	0.00	
df	62.00	
t Stat	4.22	
P(T<=t) one-tail	0.0041%	
t Critical one-tail	1.67	
P(T<=t) two-tail	0.0082%	
t Critical two-tail	2.00	

Field Validation

Five sealants (A, B, E, G and J) with previously documented field performance were installed in Montreal, Quebec, Canada in fall 1990 and were used in this study to validate the crack sealant performance criteria. The ASTM D6690 Type II test results of the five sealants are reported in Table 10 (Masson 1999). Field samples were collected during the visual survey at years 1, 3, 5, and 9. Masson et al. (1998) noted that the sealants were not always installed at the recommended pouring temperature and the air temperature and sky conditions varied (Table 11). Hence, the effect of installation needs to be considered when sealant laboratory testing results are correlated to sealant field performance.

Table 10. Montreal Sealant Standard Test Results (After Masson 1999)

Sealant	Penetration (<90 dmm)*, †	Flow (<3 mm)*	Resilience (>60%)*	Bond (3 cycles)*
A	86	0.5	57	No
B	68	0.5	64	Yes
E‡	104	1	73	Yes
G	50	0.5	51	No
J	66	6	48	Yes

*ASTM D3405 requirements. Levels beyond acceptable limits are underlined.
†1 dmm = 0.1 mm.
‡Meets ASTM D1190 specification.

The first and second performance surveys of the installed sealants were taken after three and six months of installation, and the lowest temperatures were -5°C and -35°C, respectively. The short-term performance is mostly affected by sealant installation condition and sealant stiffness. The sealant performances are shown in Table 12. For example, sealant G had 3% of the installed length de-bonded and less than 1% pull-out after one year. The de-bonding is identified as sealant loses adhesion to the crack wall and the pull-out is identified as sealant is completely absent from the crack. After first winter, sealant G de-bonding percentage increased to 24% and the pull-out percentage increased to 3%.

A long-term sealant performance survey was conducted four years after installation (Table 13). The long-term performance is mainly affected by the sealant weathering and

stiffening. A performance index (PI) was suggested based on the level of de-bonding and pull-out. The PI is calculated as follows (Masson et al., 1999):

$$PI = 100-(D+nP) \quad (19)$$

where,

PI = sealant performance index;
D = percent debonded length of the sealant;
P = percent pull-out length; and
n = an integral that accounts the effect of pull-out over de-bonding on performance

The n value was assigned 4 in Masson et al. (1999) study; the suggested value is based on the reasoning that loss of 1m of sealant may allow the intrusion of sand and stone into the pavement which can damage the pavement during its expansion and contraction (Peterson 1982). Loss of sealant also allows more water to penetrate into the pavement. This damage is more critical than de-bonding over the same length. The higher PI value, the better the sealant performance is. For example, the PI for sealant A was 33 and the performance was classified as poor; while sealant E, which was classified as good, had a PI of 72.

Table 11. Summary of Field Sealant Installations (After Masson et al., 1998)

Sealant	Temperature (°C)		Air Temperature and Weather at Start of Installation
	Recommended	Measured	
A	190-205	205	Overcast and -6°C
B	170-200	215	--
E	185-195	195	Overcast and 7°C
G	170-180	175	Overcast and 7°C
J	185-195	--	Overcast and 3°C

Table 12. Short-term Sealant Performance (Failure Lengths, %)

Sealant	Before First Winter		After First Winter	
	De-bonding	Pull-out	De-bonding	Pull-out
A	1	<1	12	9
B	5	<1	5	<1
E	1	<1	11	1
G	3	<1	24	3
J	1	<1	8	6

Table 13. Four-year Sealant Performance (Failure Lengths, %)

Sealant	De-bonding	Pull-out	Performance
A	11	14	Poor
B	22	1	Good
E	20	2	Good
G	36	14	Very Poor
J	13	12	Poor

The five Montreal sealants were then tested in the laboratory. Each sealant was tested as virgin (V, 0 year weathering), after accelerated weathering (AV, vacuum oven

aging), and after field weathering (w#, field weathering-year). Table 14 presents the CSBBR test results for the five tested Montreal sealants. Physical-chemical analysis results are also summarized and compared to low-temperature mechanical properties obtained from the CSBBR. Four physical-chemical analysis methods (gel-permeation chromatography [GPC], fourier transform infrared spectroscopy [FTIR], thermogravimetric analysis [TGA], and dynamic shear Rheometer [DSR]) were used; detailed results of the analysis are presented elsewhere (Masson et al, 2003).

Sealant A

The physical-chemical analysis shows that as sealant A oxidizes, the filler content increases, and the polymer inside sealant A forms cross-links over weathering. These factors are expected to stiffen the sealant. The polymer was also observed to break down into smaller degradation by-product, which can soften the sealant. Therefore, the mixed effect of stiffening and polymer degradation could not be predicted.

Sealant stiffness at 240s varies from 16.99MPa for the vacuum-oven aged sample to 73.84MPa for Aw9 (9-year weathering); an increase of 245%. The average creep rate (ACR) shows a trend similar to that of stiffness where the creep rate decreases with increased years of weathering. The dissipated energy ratio (DER) analysis shows that the longer the sealant is weathered, the higher the DER at the loading time of 240s. This implies that more energy was dissipated than stored with longer weathering time. However, the vacuum-aged sample shows an opposite trend from the field-weathered sealants; when stiffness decreases, ACR increases, and DER also decreases.

Sealant B

The physical-chemical analysis shows that sealant B oxidized during the installation and lost matter during weathering. Rapid oxidation occurs in the first year and after five years. A loss of heavy fraction occurred between the first and third years. The sealant's polymer was little affected by weathering.

The stiffness result shows that the virgin sealant B has a stiffness of 21.63MPa. One year after installation, the stiffness increases 103% to 44.00MPa. The stiffness decreased 28%, 8%, and 36% at years 3, 5, and 9, respectively. The ACR shows a different trend than stiffness. The highest average creep rate was determined at year 9, and the lowest creep rate was determined for the vacuum-aged sealant. The highest DER was determined when the sealant aged for five years.

Sealant E

The physical-chemical analysis of sealant E shows that polymer content has little variation during weathering. The molecular weight of bitumen of sealant E increases very slightly. This implies that sealant E has good aging characteristics and weathers very slowly. The FTIR analysis showed that sealant E had very high polymer content.

The CSBBR was unable to test sealant E due to its excessive softness. The test was conducted at -34°C first, and the beam was deflected more than the device measurement limit in less than 60s. The material was further tested at -40°C. Again, the deflection increased rapidly and was beyond the measurement capacity of the device. All virgin and weathered samples were tested; and all exceeded the CSBBR device capacity limit. This might be due to the high percentage of polymer content. According to the

manufacture data sheet, sealant E contains more than 16% SBS. Because of the high polymer content of sealant E, it is cost prohibitive and is no longer supplied by the manufacture.

Sealant G

The physical-chemical analysis of sealant G shows a large loss of bitumen due to the weathering. In the FTIR, it showed part of the sealant oxidized slowly during the first 5 years, and large sulphur oxidizes were observed. The DSR result shows that sealant has very low tanΦ, where Φ stands for phase angle, at low temperature. This means it has very little relaxation ability at low temperature.

The stiffness value of virgin sealant G was 126.27MPa and slightly decreases (5%) when the sealant was vacuum-aged. The stiffness increased 17% and 7% after 1 and 5 years of field weathering, respectively. A large increase (40%) in the stiffness was observed at Gw9 (9-year weathering). This result conflicts with the observations from the physico-chemical analysis. The lowest creep rate was determined for the vacuum-aged sample and the highest creep rate was determined for the 5-year weathered sample. However, the variation of ACR among the virgin, 1, 5, and 9-year-weathered samples is only 6%. This suggests that the sealant deflection ability does not change significantly due to weathering. The DER shows that the vacuum-aged sample had the lowest ability to dissipate energy; while the 5-year-weathered sample had the greatest ability to dissipate energy.

Sealant J

The physical-chemical analysis of sealant J showed a large portion of polymer degradation after weathering. However, the analysis also reveals up to 18 cross links per polymer chain. From the analysis, the anticipated field performance of sealant J would be softened by weathering; but still stiff due to the cross links of the polymer chain.

The stiffness of sealant J shows significant degradation. The stiffness was 454.12MPa for the virgin sealant; the stiffness drops 75%, and 84% after 1 and 3 years of field weathering, respectively. The vacuum-aged sample also shows degradation in stiffness; but only 12% decrease compared to the virgin sample. The ACR increased as stiffness decreased. The DER for the virgin and vacuum-aged samples could not be obtained because the specimen deflection was so small; and unstable data were recorded. The one-year weathered sample showed slightly better energy dissipation ability than the three-year-weathered sample.

The results in Table 14 show that VOA-aged sealants weakly correlate to field-aged Montreal sealants. For sealant A, Montreal field aged sealant shows stiffening compared to virgin sealant. However, VOA-aged sealant A shows slightly softening. Similar results were observed for sealant G. For sealant B, VOA- and Montreal field-aged sealants show the same trend; sealant became stiffer after aging. For sealant J, VOA-aged results show softening compared to virgin sealant, which is the same trend observed for the Montreal field-aged samples. However, the variation in the differences is significant.

The aforementioned discrepancy could be due to the following reasons: The samples obtained from the field had a high content of fine particles. Significant effort was spent to remove the fine particles; however, complete removal could not be achieved. This might contribute to sealant stiffening. In addition, the quantity obtained from the field is very small; therefore, sealant samples were used for more than one test. The few heating-cooling cycles might contribute to sealant softening. It is recommended that a comprehensive field survey and testing field-aged sealant be conducted.

Table 14. Test Results for Montreal Field Specimen

Sealant	Temp (°C)	S_{240} (MPa)					Avg Creep Rate	Dissipated Energy Ratio	
		Rep. 1	Rep. 2	Rep. 3	Avg	COV (%)		Ratio	Error
A_V	-34	22	21	20	21	5.7	0.30	1.3	1.0
A_AV	-34	17	17	17	17	1.7	0.33	1.2	1.0
A_w1	-34	43	40	43	42	3.7	0.29	1.4	1.0
A_w9	-34	78	74	69	74	6.6	0.28	1.6	1.0
B_V	-34	23	22	21	22	4.6	0.31	1.3	1.0
B_AV	-34	26	22	26	25	8.5	0.28	1.3	1.0
B_w1	-34	40	44	48	44	9.6	0.29	1.4	1.0
B_w3	-34	30	33	31	31	6.3	0.33	1.3	1.0
B_w5	-34	40	40	41	41	1.0	0.30	1.4	1.0
B_w9	-34	28	26	30	28	7.5	0.34	1.3	1.0
E_V	-34	Too soft to measure							
E_AV	-34								
E_w1	-34								
E_w3	-34								
E_V	-40	Too soft to measure							
E_AV	-40								
E_w1	-40								
E_w3	-40								
G_V	-34	130	121	128	126	3.5	0.23	1.8	0.1
G_AV	-34	121	124	115	120	4.1	0.19	1.1	0.4
G_w1	-34	144	151	148	148	2.5	0.21	1.2	0.6
G_w5	-34	133	135	135	135	1.0	0.23	1.8	0.2
G_w9	-34	176	176	176	176	0.1	0.20	1.3	0.3
J_V	-34	595	597	615	602	1.9	0.16	N/A	N/A
J_AV	-34	488	537	538	521	5.6	0.16	N/A	N/A
J_w1	-34	102	123	119	115	9.7	0.28	1.7	0.1
J_w3	-34	78	71	73	74	4.8	0.30	1.6	0.1

SUMMARY AND CONCLUSIONS

A modified bending beam rheometer test, crack sealant bending beam rheometer (CSBBR) was introduced. A new specimen geometry and testing procedure were developed. The CSBBR specimen, with a double thickness of the standard bending beam, was found to overcome excessive deflections during testing of bituminous crack sealants. The new beam geometry had negligible effects on the resulting deflection due to shear. In addition to changes in specimen geometry and preparation procedure, a new aging procedure, a validated testing period, and a time at which stiffness is determined were introduced. A linearity check was successfully conducted to verify that bituminous crack sealants behave as linear viscoelastic materials. The new test was found to be repeatable and the coefficient of variation between operators is less than 4%. However, significant difference was noted between devices (by different manufacturers).

The CSBBR test was found suitable to evaluate the rheological behavior of hot-poured crack sealants at low temperature. The following criteria were considered: ability to describe the sealant's rheological behavior, ease of measurement and calculation, and repeatability. Fifteen sealants were tested at a temperature range from -4°C to -40°C. Two performance parameters were identified to evaluate the crack sealants' performance at low temperature: the stiffness at 240s and the average creep rate. Both parameters are valid criteria for identifying and distinguishing among sealants. In addition, dissipated energy ratio was found to be an appropriate parameter to distinguish between sealants.

Prony series parameters that were determined using the relaxation data were successfully fitted to the viscoelastic model using a built-in module in the finite element ABAQUS software. Fitting parameters were then incorporated into a three-dimensional FE model of the CSBBR specimen. The resultant calculated creep deflections agreed with the measured values. It is concluded that Prony series expansion is adequate in describing mechanical behavior of crack sealants at low temperature. This allows the prediction of sealant behavior over longer loading time or during the unloading period.

RECOMMENDATIONS

This study recommends the implementation of CSBBR as a standard test to evaluate bituminous-based crack sealant behavior at low temperature. Two performance parameters are recommended to be determined: stiffness at 240s and average creep rate. The thresholds for the two performance parameters are maximum 25MPa and minimum 0.31, respectively. Further field validation is needed.

ACKNOWLEDGMENTS

This study is based on work supported by the Federal Highway Administration and the U.S.–Canadian Crack Sealant Consortium under pool fund award # TPF5 (045). The contribution of the participating states, industries, and provinces is greatly appreciated. The contents of this report reflect the views of the authors, who are responsible for the facts and the accuracy of the data presented herein. The content does not necessarily reflect the official views or policies of the pool fund–participating Departments of Transportation or the Federal Highway Administration. This paper does not constitute a standard, specification, or regulation.

REFERENCES

ABAQUS Finite Element Computer Program. *Theory Manual*. Version 6.5-1, Hibbit, Karlsson and Sorensen, Inc., Pawtucket, RI, USA, 2005.

Al-Qadi, I.L., Yang, S-H., Elseifi, M., Masson, J-F., and McGhee, K.M. Specifications of bituminous-based crack sealants using modified bending beam rheometer. Paper presented at the 85th Annual Meeting of the Transportation Research Board, Washington, DC, 2006.

Al-Qadi, I.L., Loulizi, A., Aref, S., Masson, J-F., and McGhee, K. M. Modification of bending beam rheometer specimen for low-temperature evaluation of bituminous crack sealants. In Transportation Research Record 1933, Transportation Research Board, Washington, DC, 2005, pp. 97-106.

Al-Qadi, I.L., Masson, J-F, Loulizi, A., Collins, P., McGhee, K.M., Woods, J., and Bundalo-Perc, S. Long-term Aging and Low Temperature Testing. Report No. B5508.5, National Research Council, Ottawa, Canada, 2003.

Al-Qadi, I.L, S-H. Yang, S. Dessouky, J-F. Masson, A. Loulizi, and M. Elseifi, "Development of Crack Sealant Bending Beam Rheometer (CSBBR) Testing to Characterize Hot-Poured Bituminous Crack Sealant at Low Temperature," In The Journal of the Association of Asphalt Paving Technologists, Vol. 76, 2007, pp. 85-122.

Anderson, D.A., Christensen, D.W., Bahia, H.U., Dongre, R., Sharma, M.G., Antle, C.E., and Button, J. Binder Characterization and Evaluation. Volume 3: Physical Characterization. SHRP-A-369 Final Report, Strategic Highway Research Program, National Research Council, Washington, DC, 1994.

Bahia, H.U., Anderson, D.A., and Christensen, D.W. The Bending Beam Rheometer: A Simple Device for Measuring Low-Temperature Rheology of Asphalt Binders. In Proceedings of the Journal of the Association of Asphalt Paving Technologists, Vol. 61, Charleston, SC, 1992, pp. 117-153.

Bahia, H.U., and Anderson, D.A. The Development of the Bending Beam Rheometer: Basics and Critical Evaluation of the Rheometer. ASTM Special Publication STP 1241. American Society for Testing and Materials, 1995, pp. 28-50.

Basu, A., Marasteanu, M.O., and Hesp, S.A.M. Time-Temperature Superposition and Physical Hardening Effects in Low-Temperature Asphalt Binder Grading. Paper Presented at the 82nd Annual Meeting of the Transportation Research Board, Washington, DC, 2003.

Belangie, M.C., and Anderson, D.I. Crack Sealing Methods and Materials for Flexible Pavements. FHWA-UT-85-1. Utah Department of Transportation, Salt Lake City, UT, 1985.

Chehovits, J., and Manning, M. Materials and methods for sealing cracks in asphalt concrete pavements. In Transportation Research Record 990. Transportation Research Record, National Research Council, Washington DC, 1984, pp. 21-30.

Chong, G.J. Rout and Seal Cracks in Flexible Pavements—A Cost-Effective Preventive Maintenance Procedure. In Transportation Research Record 1268. Transportation Research Record, National Research Council, Washington DC, 1990, pp. 8-16.

Chong, G.J. and Phang, W.A. Improved Preventive Maintenance: Sealing Cracks in Flexible Pavements in Cold Regions. Report PAV-87-01. Ontario Ministry of Transportation, Downsview, ON, 1987.

Cominsky, R.J., Huber, G.A., Kennedy, T.W., and Anderson, M. The Superpave Mix Design Manual for New Construction and Overlays. SHRP-A-407 Final Report. Strategic Highway Research Program, National Research Council, Washington, DC, 1994.

Cuelho, E., Johnson, D.R., and Freeman, R.B. Cost-Effectiveness of Crack Sealing Materials and Techniques for Asphalt Pavements. FHWA/MT-02-002/8127. Montana Department of Transportation, Helena, MT, 2002, 247 pp.

Cuelho, E., Ganeshan, S.K., Johnson, D.R., Freeman, R.B., and Schillings, P.L. Relative Performance of Crack Sealing Materials and Techniques for Asphalt Pavements. Third International Symposium on Maintenance and Rehabilitation of Pavements and Technological Control, Guimarães, Portugal, July 7–10, 2003, pp. 327–337.

Eaton, R.A., and Ashcraft, J. State-of-the-Art Survey of Flexible Pavement Crack Sealing Procedures in the United States. Report 92-18. Cold Regions Research & Engineering Laboratory, U.S. Army Corps of Engineers, Hanover, NH, 1992.

Elseifi, M., Dessouky, S., Al-Qadi, I.L., and Yang, S.H. A Viscoelastic Model to Describe the Mechanical Response of Bituminous Sealants at Low Temperature. Presented at the 85th Annual Meeting of the Transportation Research Board, Washington, DC, 2006.

Fang, C., Galal, K.A., Ward, D.R., Haddock, J.E., and Kuczek, T. Cost-Effectiveness of Joint and Crack Sealing. Presented at the 82nd Annual Meeting of the Transportation Research Board, Washington, DC, 2003.

Ferry, J.D. Viscoelastic Properties of Polymers. 3rd Ed, Wiley, New York, 1980.

Findley, W.N., Lai, J.S., and Onaran, K. Creep and Relaxation of Nonlinear Viscoelastic Materials. North Holland, Amsterdam, 1976.

Hesp, S.A.M. An Improved Low-Temperature Asphalt Binder Specification Method. Final. MTO Contract No. 9015-A-000190 and NCHRP-IDEA Contract No. 84, Kingston, Ontario, 2004.

Hills, J.F. and Brien, D. The Fracture of Bitumens and Asphalt Mixes by Temperature Induced Stresses. In Proceedings of the Journal of Association of Asphalt Paving Technologists Vol. 35, 1966, pp. 292–309.

Ho, S.M.S., and Zanzotto, L. Sample Preparation for Direct Tension Testing – Improving Determination of Asphalt Binder Failure Stress and Test Repeatability. In Transportation Research Record 1766. Transportation Research Board, Washington, DC, 2000, pp. 15-23.

Johansson, L.S. and Isacsson, U. Effect of Filler on Low Temperature Physical Hardening of Bitumen. Construction and Building Materials, Vol. 12, 1998, pp. 463-470.

Joseph, P. Field Evaluation of Rout and Seal Crack Treatment in Flexible Pavement. Report PAV-90-03, Ministry of Transportation of Ontario, Downsview, ON, 1990.

Ketcham, S. Sealants and Cold Regions Pavement Seals. CRREL Report 95-11, U.S. Army Corps of Engineers, 1995.

Khuri, M.F., and Tons, E. Comparing rectangular and trapezoidal seals using the finite element method. In Transportation Research Record 1334. Transportation Research Board, Washington, DC, 1993, pp. 25-37.

Kim, Y.R. and Little, D.N. Linear viscoelastic analysis of asphalt mastics. Journal of Materials in Civil Engineering, ASCE, Vol. 16, No. 2, 2004, pp. 122-132.

Linde, S. Investigations on the Cracking Behavior of Joints in Airfields and Roads: Field Investigations and Laboratory Simulation. SP Report 1988:23. Swedish National Testing Institute, Borås, Sweden, 1988.

Lundström, R. and Isacsson, U. Linear Viscoelastic and Fatigue Characteristics of Styrene-Butadiene-Styrene Modified Asphalt Mixtures ASCE, Journal of Materials in Civil Engineering Vol.16, No. 6, 2004, pp.629-638.

Marasteanu, M.O., and Anderson, D.A. Establishing linear viscoelastic conditions for asphalt binders. In Transportation Research Record 1728. Transportation Research Board, Washington, DC, 2000, pp. 1-6.

Masson, J.-F. Bituminous Sealants for Pavement Joints and Cracks: Building the Basis for a Performance-Based Specification. In Durability of Building and Construction Sealants. A. Wolf, Ed., RILEM, Paris, 2000, pp. 315-328.

Masson, J.-F., Collins, P., and Légaré, P.P. Performance of pavement crack sealants in cold urban conditions. In Canadian Journal of Civil Engineering, Vol. 26, No. 4, 1999, pp. 395-401.

Masson, J-F., Collins, P., Margeson, J., and Polomark, G. Analysis of bituminous crack sealants by physicochemical methods: relationship to field performance. In Transportation Research Record 1795, Transportation Research Board, Washington, DC, 2002, pp. 33-39.

Masson, J.-F and Lacasse, M.A. Considerations for a Performance-Based Specification for Bituminous Crack Sealants. In Flexible Pavement Rehabilitation and Maintenance, ASTM Special Publication STP1348. American Society for Testing and Materials, 1998.

Masson, J.-F., and Lacasse, M.A. Effect of Hot-Air Lance on Crack Sealant Adhesion. Journal of Transportation Engineering. ASCE, Vol. 125, No. 4, 1999, pp. 357-363.

Masson, J-F., Collins, P., Bundalo-Perc, S., Woods, J.R., and Al-Qadi, I.L. “Accelerated Aging of Bituminous Sealants: Small-kettle Aging,” 86th TRB Annual Meetings, Paper No. 07-1520, Washington D.C., January 21-25, 2007.

Masson, J-F., Collins, P., Bundalo-Perc, S., Woods, J.R., and Al-Qadi, I.L. “Early Thermodegradation of Bituminous Sealants Resulting from Improper Installation: Field Study,” In Journal of the Transportation Research Record, No. 1991, Transportation Research Board of the National Academies, Washington, DC, Oct 2007, pp. 119-123.

Park, S.W., and Schapery, R.A. Methods of Interconversion between Linear Viscoelastic Material Functions. Part I—a numerical method based on Prony series. International Journal of Solids and Structures, Vol. 36, 1999, pp. 1653-1675.

Park, S.W., and Kim, Y.R. Fitting Prony-Series Viscoelastic Models with Power-Law Presmoothing. In Journal of Materials in Civil Engineering, ASCE, Vol. 13, No. 1, 2001, pp. 26-32.

Petersen, J.C., Robertson, R.E., Branthaver, J.F., Harnsberger, P.M., Duval J.J., Kim, S.S., Anderson, D.A., Christiansen, D.W., Bahia, H.U., Dongre, R., Antle, C.E., Sharma, M.G., Button, J.W., and Glover, C.J. Binder Evaluation and Characterization – Volume 4: Test Methods. SHRP-A-370 Final Report, Strategic Highway Research Program, National Research Council, Washington, DC, 1994.

Readshaw, E.E. Asphalt specifications in British Columbia for low temperature performance. In Proceedings of the Association of Asphalt Paving Technologists, Vol. 42, 1972, pp. 562-581.

Schapery, R.A. and Park, S.W. Methods of interconversion between linear viscoelastic material functions, Part II—an approximate analytical method. International Journal of Solids and Structures, Vol. 36, No.11, 1999, pp. 1677-1699.

Smith, K.L., and Romine, A.R. Innovative Materials Development and Testing Volume 3: Treatment of Cracks in Asphalt Concrete-Surfaced Pavements. SHRP-H-354. Strategic Highway Research Program, National Research Council, Washington, DC, 1993.

Smith, K.L., and Romine, A.R. LTPP Pavement Maintenance Materials: SHRP Crack Treatment Experiment. FHWA-RD-99-143, Final Report. FHWA, Washington, DC, 1999, 163 pp.

Treloar, L.R.G. The Elasticity and Related Properties of Rubbers. Rubber Chemistry and Technology, Vol. 47, 1974, pp. 625–696.

Ward, D.R. Evaluation of the Implementation of Hot-Pour Sealants and Equipment for Crack Sealing in Indiana. FHWA/IN/JTRP-2000/27, FHWA, Washington, DC, 2001, 189 pp.

Zanzotto, L. Laboratory Testing of Crack Sealing Materials for Flexible Pavements. Final Report. Transportation Association of Canada, Ottawa, ON, 1996.

Zhang, X., and Huber, G. Effect of Asphalt Binder on Pavement Performance: An Investigation Using the SuperPave Mix Design System. In Proceedings of the Association of Asphalt Paving Technologists, Vol. 65, 1996, pp. 449-490.

APPENDIX A: CSBBR TESTING PROCEDURE

Step 1: Obtain test sample from freezer and place on a lab table 12-24 hrs before testing. This allows the sample to adjust to ambient temperature.

Step 2: Heat oven A to recommended installation temperature.

Step 3: Spray release agent onto test sample mold.

Step 4: Use 50mm binder clips to hold mold pieces into shape.

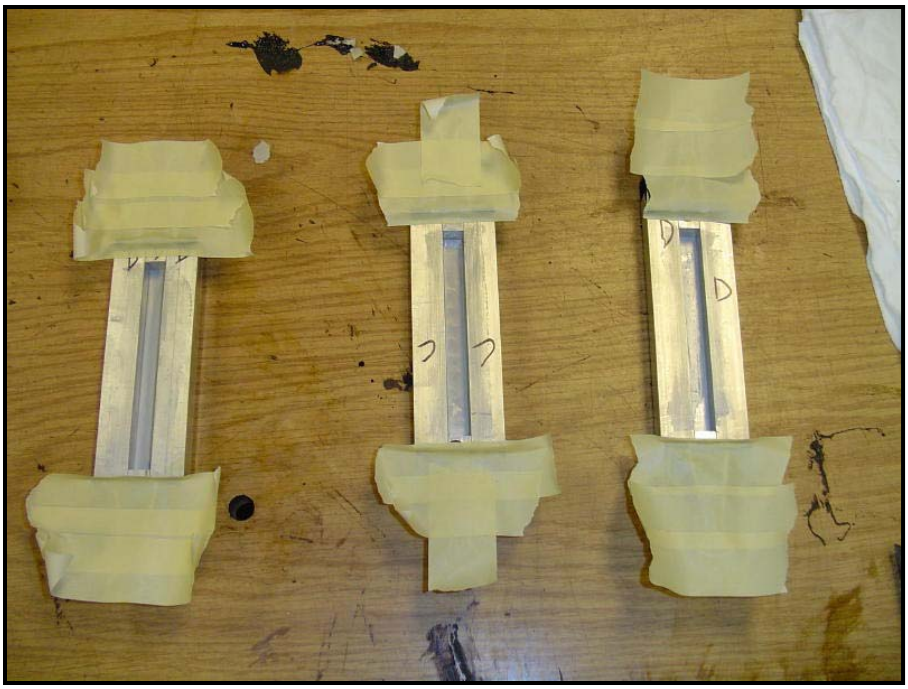

Step 5: Use general purpose masking tape to cover the clamps holding the test mold.

Step 6: Place test samples into oven A for 30mins.

Step 7: After 15min of placing sealant into oven A, place empty mold on the ceramic tile in oven B; the tile is preheated to 50°C lower than recommended sealant installation temperature for 15mins.

Step 8: Fifteen min after placing test samples into heated oven, stir the samples to ensure the sample is thoroughly mixed. Scrape the bottom and sides of the canister. Place the test samples back into the oven for the remaining 15mins.

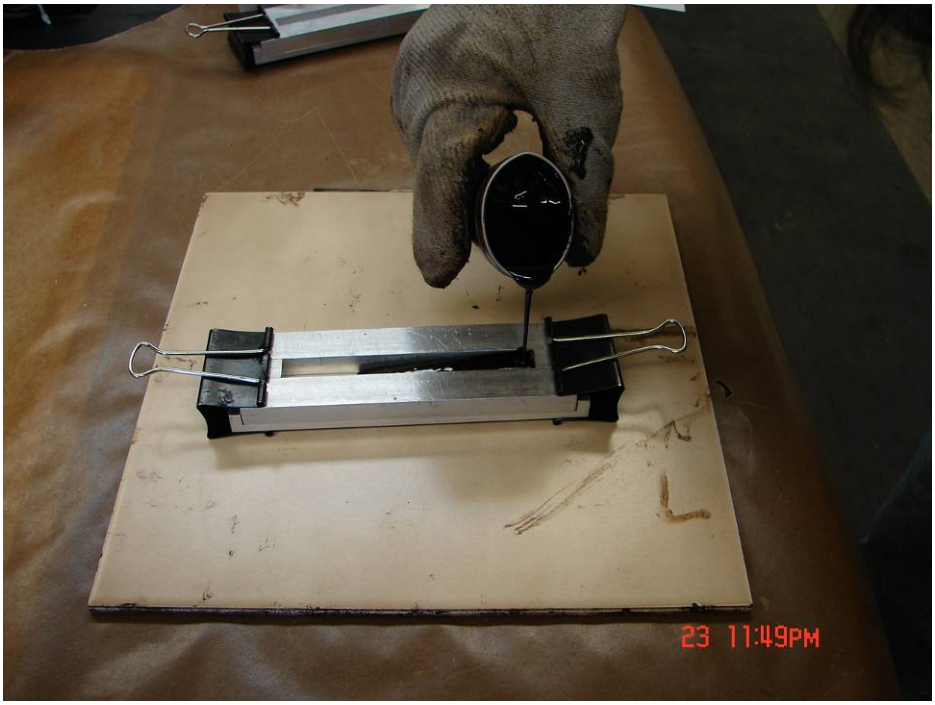

Step 9: Pour the sealant material in the preheated mold that has been placed on the ceramic tile. This prevents sealant material from cooling down rapidly. Start from one end of the mold and proceed slowly towards the opposite end.

Step 10: Allow the test specimens to cool for 1hr.

Step 11: Use a propane blow torch to heat a cutting knife.

Step 12: Angle the mold downward and trim the excess sealant from the test mold.

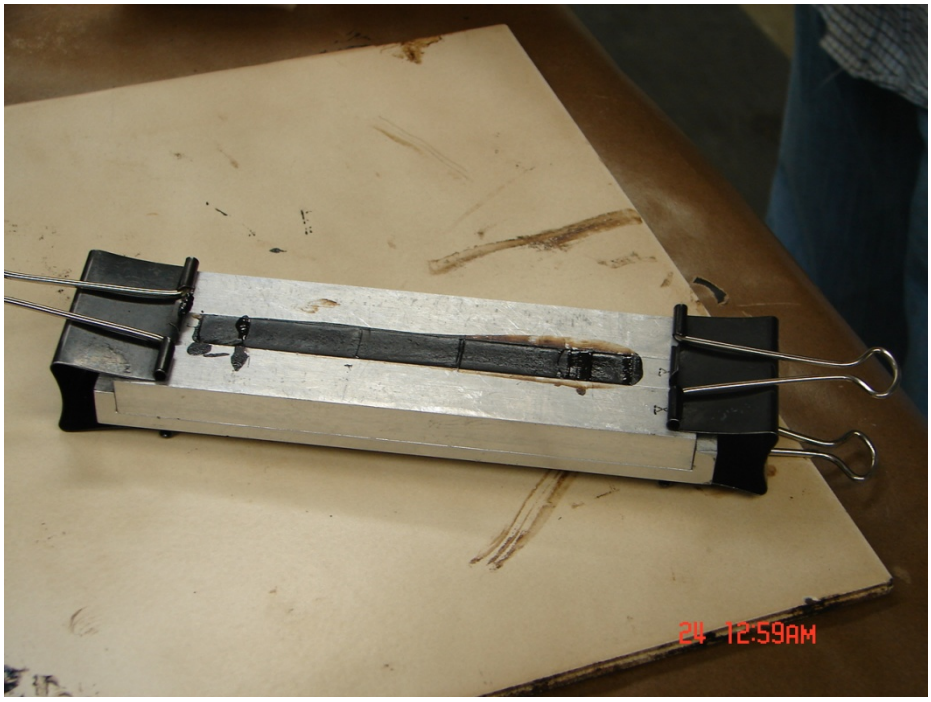

Step 13: Specimens should be flushed with the top of the mold without any visible deformation. Unclamp the mold.

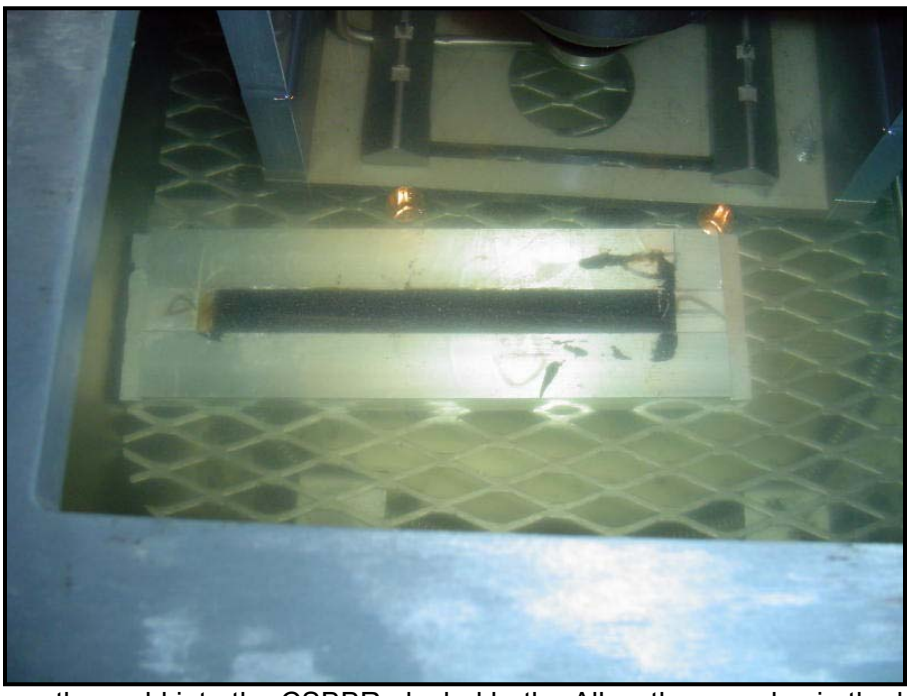

Step 14: Place the mold into the CSBBR alcohol bath. Allow the samples in the bath for one minute.

Step 15: Take out the mold and place it on a flat surface to remove the sealant from the mold.

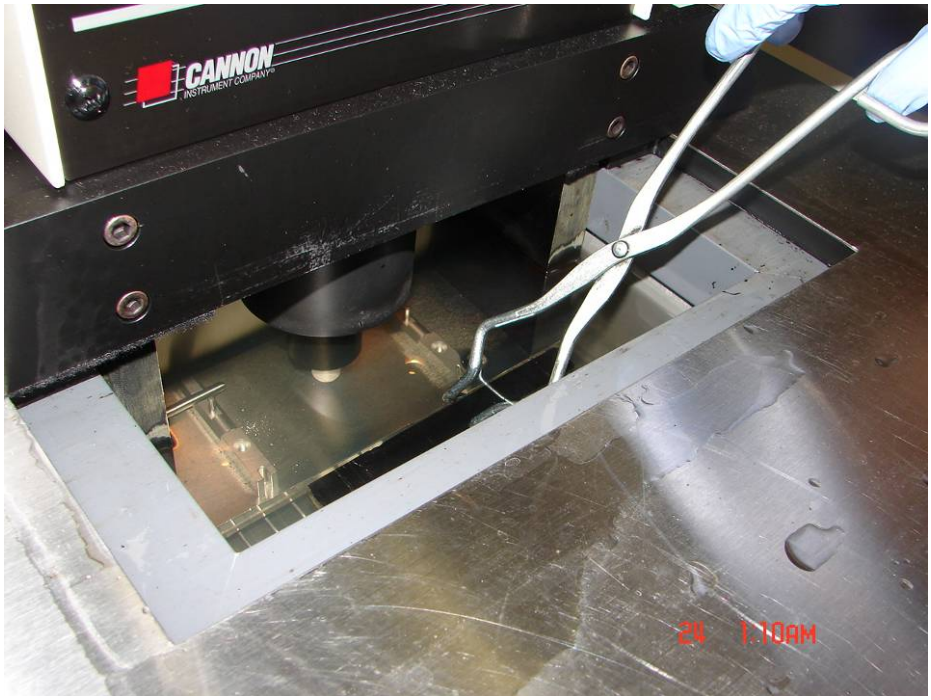

Step 16: Place the specimen in the bath for 1hr; and then proceed with testing.

APPENDIX B: SPECIMEN SIZE EFFECT OF BENDING BEAM RHEOMETER

To determine the percentage of the deflection due to shear, the virtual work method was used. To determine maximum deflection at the midspan of a beam, a unit virtual force is applied at the center of the beam (Figure B-1a). The resultant virtual shear, v, and virtual moment, m, are shown in Figure B-1b and c, respectively. When the real force is applied (Figure B-1d), it induces real shear forces, V, and real moments, M (Figure B-1e and f, respectively).

If the beam is dx units long, dy units wide, and dz units high, the internal work, du_1, produced by the virtual moments, m, due to the action of the real load is given as follows:

$$du_1 = \frac{mMdx}{EI} \tag{B-1}$$

where E is the elastic modulus and I is the moment of inertia. The internal work, du_2, obtained by the virtual shear, □*, due to the shearing forces (□) of the real load is as follows:

$$du_2 = \frac{\tau^* \tau}{G} dxdydz \tag{B-2}$$

where G is the shear modulus, which is related to the elastic modulus:

$$G = \frac{E}{2(1+\nu)} \tag{B-3}$$

where □ is the Poisson's ratio. The external work done by the virtual load due to the application of the actual load is equal to 1 times w_0, where w_0 is the center deflection. The external work done by the virtual load must equal the internal work done by the virtual moments and virtual shear stresses, which can be written as follows:

$$1 \; x \; w_0 = \int_0^L \frac{mM}{EI} dx + \int_{-h/2}^{h/2} \int_0^b \int_0^l \frac{\tau^* \tau}{G} dxdydz \tag{B-4}$$

where h is the beam thickness, b is the beam width, and l is the beam length. For a beam, shear stresses are distributed according to a parabola, as presented by Equation B-5:

$$\tau = (\frac{V}{2I})((\frac{h}{2})^2 - z^2) \tag{B-5}$$

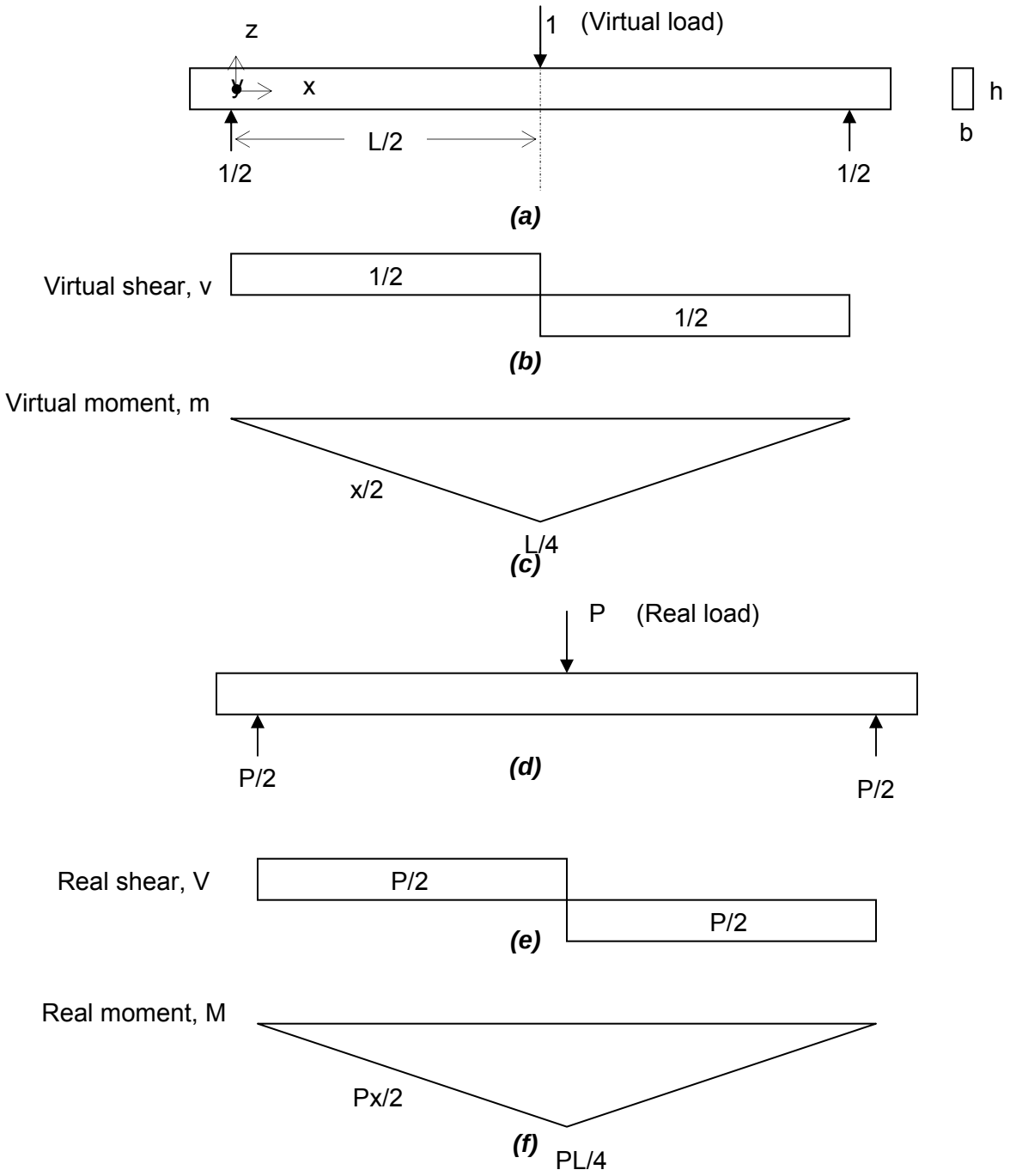

Figure B-1. Virtual Work Method to Evaluate Maximum Deflection at Midspan of a Beam.

Using the shear diagrams presented in Figure B-1b and e, the virtual and actual shear stresses are given by Equations (B-6) and (B-7), respectively:

$$\tau^* = (\frac{1}{4I})((\frac{h}{2})^2 - z^2) \qquad \text{(B-6)}$$

$$\tau = (\frac{P}{4I})((\frac{h}{2})^2 - z^2) \quad \text{(B-7)}$$

Noting that the loading is symmetric with respect to the center of the beam and that the shear stress is distributed symmetrically with respect to the top and bottom of the beam, and using Equations B-6 and B-7, Equation B-4 can be written as follows:

$$w_0 = \frac{2}{EI}\int_0^{L/2} \frac{x}{2}\frac{Px}{2}dx + \frac{2b}{G}\int_0^{L/2} dx 2\int_0^{h/2} \frac{1}{4I}\frac{P}{4I}((\frac{h}{2})^2 - z^2)^2 dz \quad \text{(B-8)}$$

From Equation B-8,

$$w_0 = \frac{PL^3}{48EI} + \frac{3PL}{10Gbh} \quad \text{(B-9)}$$

The first term in Equation B-9 represents the deflection due to bending. The second term in Equation B-9 represents the deflection due to shear. Equation B-9 can also be written as shown by Equations B-10 through B-13:

$$w_0 = \frac{PL^3}{48EI} + \frac{3PL(1+\nu)}{5EA} \quad \text{(B-10)}$$

$$w_0 = \frac{PL^3}{48EI} + \frac{3PL(1+\nu)}{5Ebh} \quad \text{(B-11)}$$

$$w_0 = \frac{PL^3}{48EI} + \frac{PLh^2(1+\nu)}{20EI} \quad \text{(B-12)}$$

$$w_0 = \frac{PL^3}{48EI}(1 + \frac{12h^2(1+\nu)}{5L^2}) \quad \text{(B-13)}$$

Equation B-13 shows that when the length of the beam is much greater than its thickness, the term in the bracket approaches a unit value, which means that shear effects are minimal. The beam size used for asphalt binder testing is 102mm long and 6.35mm high. Assuming a Poisson's ratio of 0.15, the term between brackets in Equation B-13 would equal 1.01, which means that shear effects contribute only 1% to the center deflection, which is negligible. For the new beam dimension, the thickness is 12.7mm, and for a Poisson's ratio of 0.15, the term between brackets in Equation B-13 would be equal to 1.04, which means that the shear effects contribute to only 4% to the center deflection, which is deemed acceptable.

APPENDIX C: TEST SPECIFICATION

Method to Measure Low Temperature Flexural Creep Stiffness of Bituminous Sealants and Fillers by Bending Beam Rheometer (BBR)
Sealant Consortium Designation: SC-5

1. SCOPE

1.1. This method applies to bituminous sealants used in the construction and maintenance of roadways.

1.2. The method is used to determine the bituminous sealant flexural stiffness. It can be used on unaged material or on material aged using Test Method SC-3 (Vacuum Oven Aging). The test apparatus is designed for testing within the temperature range from -4°C to -40°C.

1.3. The values stated in SI units are to be regarded as the standard.

1.4. This practice covers the determination of flexural stiffness in bituminous sealants using the bending beam rheometer and by conducting the creep test.

2. REFERENCED DOCUMENTS

2.1. AASHTO Standards:

T313, Determining the Flexural Creep Stiffness of Asphalt Binder Using the Bending Beam Rheometer (BBR).

2.2. ASTM Standards

- D6648-01, Standard Test Method for Determining the Flexural Creep Stiffness of Asphalt Binder Using the Bending Beam Rheometer (BBR).
- D5167-03, Standard Practice for Melting Hot-Applied Joint and Crack Sealant and Filler for Evaluation.
- D6373-99, Standard Specification for Performance Graded Asphalt Binder.
- E77-98(2003), Test Method for the Inspection and Verification of Thermometers.
- E145-94(2006), Standard Specification for Gravity-Convection and Forced-Ventilation Ovens.
- E1-05 Standard Specifications for ASTM Liquid-in-Glass Thermometers

2.3. Documents of the Sealant Consortium (SC):

- SC-1, Guidelines for Graded Bituminous Sealants.
- SC-2, Test Method for Measuring Apparent Viscosity of Hot-poured Crack Sealant Using Brookfield Rotational Viscometer RV Series Instrument
- SC-3, Method for the Accelerated Aging of Bituminous Sealants.
- SC-4, Method to Evaluation of the Tracking Resistance of Bituminous Sealants and Fillers by Dynamic Shear Rheometry.

- SC-5, Method to Measure Low Temperature Sealant Flexural Creep Stiffness at Low Temperature by Bending Beam Rheometer.
- SC-6, Method to Evaluate Sealant Extensibility at Low Temperature by Direct Tension Test.
- SC-7, Blister Method to Measure the Adhesion of Bituminous Sealants.

3. TERMINOLOGY

3.1. Bituminous sealants are hot-poured modified asphaltic materials used in pavement cracks and joints.

3.2. Definitions of Terms Specific to This Standard:

3.2.1 Contact load, n – the load, Pc, required to maintain positive contact between the test specimen, supports, and the loading shaft; 35 ± 10mN.

3.2.2 Flexural creep compliance, D(t), n – the ratio obtained by dividing the maximum bending strain in a beam by the maximum bending stress. The flexural creep stiffness is the inverse of the flexural creep compliance.

3.2.3 Flexural creep stiffness, S(t), n – the creep stiffness obtained by fitting a second order polynomial to the logarithm of the measured stiffness at 8.0, 15.0, 30.0 60.0, 120.0, and 240.0s and the logarithm of time.

3.2.4 Measured flexural creep stiffness, Sm (t), n – the ratio obtained by dividing the measured maximum bending stress by the measured maximum bending strain. Flexural creep stiffness has been used historically in asphalt technology while creep compliance is commonly used in studies of viscoelasticity.

3.2.5 Average creep rate – the average creep rate obtained by fitting the power law model of the logarithm of the strain versus the logarithm of time. The average creep rate is the absolute value of the exponents of the power law model.

3.2.6 Test load, n – the load, Pt, of 240s duration is used to determine the stiffness of the crack sealant being tested; 980 ± 50mN.

4. SUMMARY OF PRACTICE

4.1. The bending beam rheometer is used to measure the midpoint deflection of a simply supported prismatic beam of bituminous crack sealant subjected to a constant load applied to the midpoint of the test specimen. The device operates only in the loading mode.

4.2. A prismatic test specimen is placed in the controlled temperature fluid bath and loaded with a constant test load for 240.0s and unloaded for 480.0s. The test load (980 ± 50mN) and the midpoint deflection of the test specimen are monitored versus time using a computerized data acquisition system.

5. SIGNIFICANCE AND USE

5.1. This test is intended for bituminous sealants applied to roadway joints and cracks.

5.2. The test temperature is determined as the lowest temperature experienced by the pavement surface in the geographical area for which the sealant is intended.

5.3. The flexural creep stiffness or flexural creep compliance, determined from this test, describes the low-temperature stress-strain-time response of crack sealant at the test temperature.

5.4. The average creep rate determined from this test gives an indication of the rate of deformation of crack sealant at the test temperature.

5.5. Sealants must be homogenized before being used to conduct this test.

6. APPARATUS

6.1. A crack sealant bending beam rheometer (CSBBR) test system consists of the following: (1) a modified bending beam rheometer with a controlled temperature liquid bath which maintains the test specimen at the test temperature, (2) test specimen molds, and (3) items for verifying and calibrating the system.

6.2. A Modified Bending Beam Rheometer – A CSBBR is modified from a typical BBR. The CSBBR has a modified loading frame system which can accommodate a specimen 12.7mm in height to operate a three-point bending beam test that applies a constant test load for 240.0s and unloads for 480.0s The specification required by the CSBBR system is in accordance with Test Method T313. The updated version software can be obtained from the instrument manufactures.

6.3. Test Specimen Molds – Test specimen molds with interior dimensions of 12.70 ± 0.05mm wide by 12.70 ± 0.05mm deep by 102.0 ± 0.5mm long fabricated from aluminum or stainless steel (Figure 1).

6.3.1 The thickness of the two spacers used for each mold (small end pieces used in the metal molds) shall be measured with a micrometer and shall not vary from each other in thickness by more than 0.05mm.

NOTE 1 – Small errors in the thickness of the test specimen can have a significant effect on the calculated stiffness because the calculated stiffness is a function of the thickness, h, raised to the third power.

6.4. Items for Calibration – items remain the same as AASHTO Test Method T313, except the dimension of the stainless steel (thick) beam use for calibration. The new calibration kits can be obtained from the instrument manufactures.

6.5. Calibrated Thermometers – calibrated liquid-in-glass thermometers to verify the temperature transducer of suitable range with subdivisions of 0.1°C.

6.6. Laboratory Ovens – two standard laboratory ovens capable of producing and maintaining a temperature of 200 ± 0.5°C.

7. REAGENTS AND MATERIALS

7.1. Bath Fluid – A bath fluid that is not absorbed by or does not affect the properties of the crack sealant being tested. The bath fluid shall be optically clear at the test temperature.

7.2. Binder Clip – A binder clip is used to hold the aluminum mold to maintain the size of the sample to prevent shrinkage during sealant cooling.

7.3. Release Agent – A proper release agent prevents bituminous crack sealant from sticking to the mold. Using a spray type silicon-based release agent is recommended.

7.4. Solvent – A solvent can properly clean the molds, end tabs, and plates. The parts cleaned by the solvent shall be submerged in the ethanol prior to use. Cleaning ensures the proper bond between sealant and end tabs.

7.5. Cleaning Cloths – Cloths for wiping molds, end tabs and plates.

8. HAZARDS

8.1. Standard laboratory caution should be used in handling hot bituminous sealant in accordance with ASTM D5167, and required safety procedures should be followed when chemical agents are used.

9. VERIFICATION AND CALIBRATION

9.1. BBR – Follow the procedure as stated in AASHTO T313.

9.2. Oven and freezer – Calibrate the temperature with a thermometer that meets the requirements of ASTM E1. The thermometer calibration can be verified according to ASTM E77.

10. SAMPLES PREPARATION

10.1. Preparation of Molds.

10.1.1 Spread a very thin layer of release agent on the interior faces of four mold sections to prevent the crack sealant from sticking to the metal end pieces. Assemble the mold and use binder clips to hold the pieces of the mold together.

10.1.2 Preheat the oven to a temperature 50°C lower than recommended pouring temperature at least one hour before testing. Place the mold on the ceramic tiles into the oven 15mins before pouring the crack sealant.

10.2. Preparation of Test Specimens.

10.2.1 Laboratory-aged samples shall be obtained in accordance with appropriate test methods.

10.2.2 Heat 4 cans of bituminous crack sealant, which contain 35g of bituminous sealant each, in an oven set at the sealant manufacturer-recommended pouring temperature until the sealant is sufficiently fluid to pour (Do not heat the sealant more than 30mins.) Each can of sealant will be poured into its own mold.

10.3. Molding Test Specimens – 4 replicates should be prepared for each tested sealant. Prior to pouring the sealant, take one preheated mold and one ceramic tile from the oven. With the preheated mold on the ceramic tile, firmly stir the sealants prior to pouring into the molds to ensure the homogeneity of the sealant. Begin pouring the sealant from one end of the mold and move toward the other end, slightly overfilling the mold. When pouring, hold the sample container 20 to 30mm from the top of the mold, pouring continuously toward the other end in a single pass. Repeat the same procedure for the other three molds. Place the filled mold on the preheated ceramic tile and allow the mold to cool for one hour to room temperature. After cooling to room temperature, trim the exposed face of the cooled specimens even with the top of the mold using a hot knife.

10.4. Storing and Demolding Test Specimens.

10.4.1 Store all test specimens in their molds at room temperature prior to testing. Testing shall be completed within 4hrs after specimens are poured.

10.4.2 Just prior to demolding, cool the molds containing the test specimens in a cold fluid bath which has the same temperature as the selected test temperature for no longer than 5min, but only long enough to stiffen the test specimen so that it can be readily demolded without distortion. A 15-minute interval between each sample is desired prior to placing the sample into the cold chamber bath. Do not cool the molds containing the specimens in the test bath because it may cause temperature fluctuations in the bath to exceed ± 0.2°C.

10.4.3 Immediately demold the specimen when it is sufficiently stiff to demold without distortion, by disassembling the mold. To avoid distorting the specimen, demold the specimen by sliding the metal side pieces from the specimen.

NOTE 2 – During demolding, handle the specimen with care to prevent distortion. Full contact at specimen supports is assumed in the analysis. A warped test specimen may affect the measured stiffness.

11. PROCEDURE

11.1. All sealants to be tested must undergo the aging process. Follow the procedure described SC-3, Method for the Accelerated Aging of Bituminous Sealants It is recommended that a minimum of 150g of bituminous sealant be prepared for a set of tests.

11.2. Select the appropriate test temperature for the crack sealant specimen. After demolding, immediately place the test specimen in the testing bath and condition it at the testing temperature. The test specimen shall remain submerged in the bath fluid at the test temperature ± 0.1°C for the entire 60 ± 5min.

11.3. Check the adjustment of the contact load and test load prior to testing each set of test specimens. The 12.7-mm thick stainless steel beam shall be used for checking the contact load and test load.

11.3.1 Place the 12.7mm steel beam in position on the beam supports. Using the test load regulator valve, gently increase the force on the beam to 980 ± 50mN.

11.3.2 Switch from the test load to the contact load and adjust the force on the beam to 35±10mN. Switch between the test load and contact load four times to ensure that the load is stable.

11.3.3 When switching between the test load and contact load, watch the loading shaft and platform for visible vertical movement. The loading shaft shall maintain contact with the steel beam when switching between the contact load and test load, and the contact load and test load shall be maintained at 35±10mN and 980±50mN, respectively.

11.4. Enter the specimen identification information, including the elapsed time the specimen has been conditioned in bath at the test temperature, and other information as appropriate into the computer that controls the test system.

11.5. After conditioning, place the test specimen on the test supports and gently position the back side of the test specimen against the alignment pins. Initiate the test.

11.6. The bath temperature shall be maintained at the selected test temperature ± 0.1°C during the test; otherwise the test shall be rejected.

11.7. The contact load shall be applied by gently increasing the load to 35±10mN. While applying the contact load, the load on the beam shall not exceed 45mN, and the time to apply and adjust the contact load shall be no greater than 10s.

11.8. With the contact load applied to the test specimen, activate the automatic test system, which is programmed to proceed as follows:

11.8.1 Apply a 980±50mN seating load for 1±0.1s.

11.8.2 Reduce the load to the 35±10mN contact load and allow the test specimen to recover for 480±0.1s. At the end of the test, the operator shall monitor the computer screen to verify that the load on the test specimen returns to 35±10mN. If it does not, the test shall be rejected.

11.8.3 Apply a 980±50mN test load to the test specimen. The software shall record the test load at 0.5-second intervals from 0.5 to 240s and calculate the average

of the recorded load values. Between 0.5 and 5s, the test load shall be within ±50mN of the average test load and for the remaining times within ±10mN of the average test load. The actual load on the test specimen as measured by the load cell shall be used to calculate the stress in the test specimen.

11.8.4 Remove the test load and return to the 35 ± 10mN contact load and collect the data for 480s.

11.8.5 Remove the specimen from the supports and proceed to the next test.

12. CALCULATIONS

12.1. Deflection of an Elastic Beam – Using the elementary bending theory, the midspan deflection of an elastic prismatic beam of constant cross-section loaded in three-point loading can be obtained by applying Equations 12.1 and 12.2 as follows:

$$\delta = PL^3/48EI \qquad (12.1)$$

where:

δ = deflection of beam at midspan, mm,
P = load applied, N,
L = span length, mm,
E = modulus of elasticity, MPa, and
I = moment of inertia, mm^4.

$$I = bh^3/12 \qquad (12.2)$$

where:

b = width of beam, mm, and
h = thickness of beam, mm.

NOTE – The test specimen has a span to depth ratio of 10 to 1, and the contribution of shear to deflection of the beam can be neglected.

12.2. Elastic Flexural Modulus – According to elastic theory, calculates the flexural modulus of a prismatic beam of constant cross-section loaded at its midspan. Therefore:

$$E = PL^3/4bh^3 \qquad (12.3)$$

where:

E = flexural creep stiffness, MPa,
P = load, N,
L = span length, mm,
b = width of beam, mm,
h = depth of beam, mm, and
δ = deflection of beam, mm.

12.3. Maximum Bending Stress – the maximum bending stress occurs at the top and bottom of the beam at its midspan. Therefore:

$$\sigma = 3PL/2bh^2 \qquad (12.4)$$

where:

σ = maximum bending stress in beam, MPa,
P = constant load, N,
L = span length, mm,
b = width of beam, mm, and
h = depth of beam, mm.

12.4. Maximum Bending Strain – the maximum bending strain in the beam occurs at the top and bottom of the beam at its midspan. Therefore:

$$\varepsilon = 6\delta h/L^2 \text{ mm/mm} \qquad (12.5)$$

where:

ε = maximum bending strain in beam, mm/mm,
δ = deflection of beam, mm,
h = thickness of beam, mm, and
L = span length, mm.

12.5. Linear Viscoelastic Stiffness Modulus – According to the elastic-viscoelastic correspondence principle, it can be assumed that if a linear viscoelastic beam is subjected to a constant load applied at t = 0 and held constant, the stress distribution in the beam would be the same as that in a linear elastic beam under the same load. Further, the strains and displacements depend on time and are derived from those of the elastic case by replacing E with 1/D(t). Since 1/D(t) is numerically equivalent to S(t), rearranging the elastic solution results in the following relationship for stiffness:

$$S(t) = PL^3/4bh^3\delta(t) \qquad (12.6)$$

where:

S(t) = time-dependent flexural creep stiffness, MPa,
P = constant load, N,
L = span length, mm,
b = width of beam, mm,
h = depth of beam, mm,
δ(t) = deflection of beam, at time t, mm, and

δ(t) and S(t) indicate that the deflection and stiffness, respectively, are functions of time.

12.6. Average Creep Rate – Average Creep Rate is obtained by dividing the cumulative creep strain by the cumulative time for the 240s loading period. The strain versus time data is plotted in the log-log scale (Figure 2). The obtained curve is fitted into the power law:

$$\varepsilon(t) = A(t)^N \qquad (12.6)$$

where:

ε (t) = strain; and

N = Average creep rate.

13. REPORT

13.1. Report the following information: sealant name and supplier, test sample ID, date of aging (dd/mm/yy), date of test (dd/mm/yy), time of demolding (h, m), time of conditioning (h, m), time test load applied for each sample (h, m), test temperature, maximum and minimum temperature during the test, any deviations from test load and temperature, measured stiffness modulus and average creep rate.

14. PRECISION AND BIAS

14.1. Confidence intervals of 95% should be constructed around the average of the calculated stiffness from the results of the four replicates. The closest three measurements will then be used to calculate the coefficient of variation while the fourth replicate will be discarded. A coefficient of variation less than 10% is desirable.

15. KEYWORDS

15.1. Hot-poured bituminous sealant; joint; crack; direct tension test; stiffness; average creep rate; creep compliance.

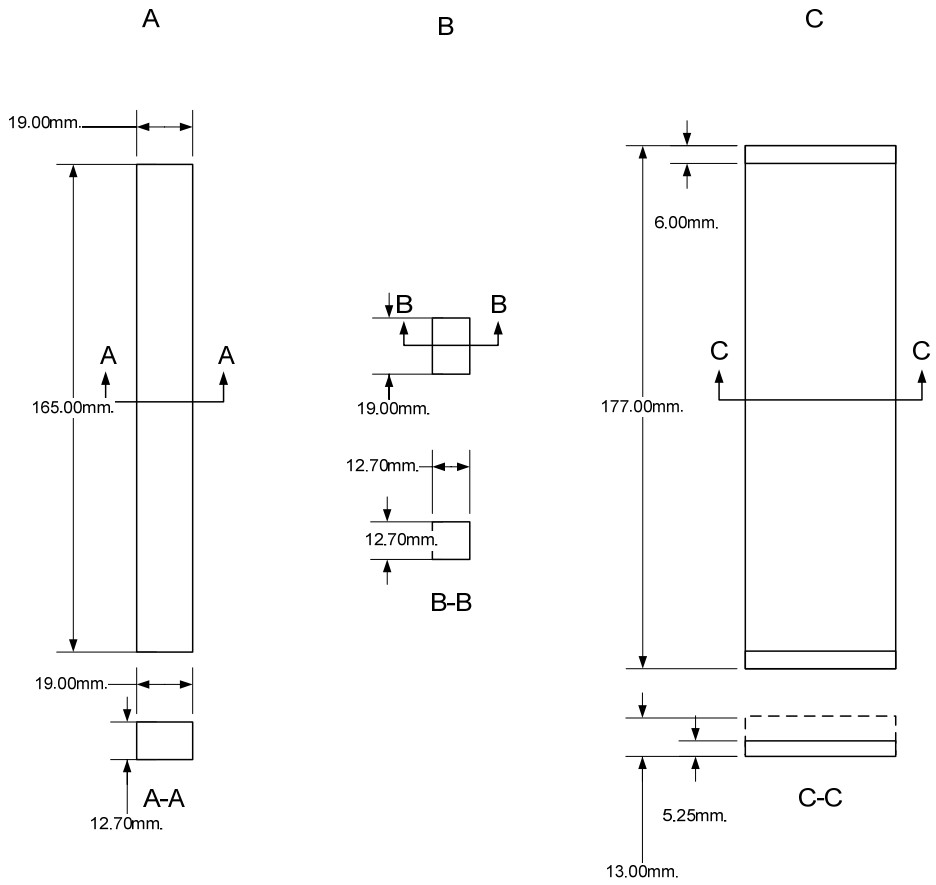

IT	QTY	DESCRIPTION
A	2	Side Bar
B	2	Spacer Bar
C	1	Bottom Plate

Figure 1. Dimension for crack sealant Bending Beam Rheometer mold and modified specimen support

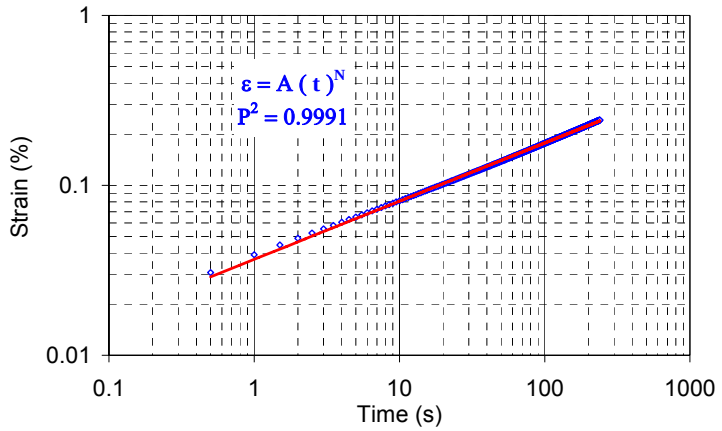

Figure 2. Strain versus time plotted in the log-log scale and used to calculate average creep rate


Illinois Department
of Transportation


ILLINOIS
UNIVERSITY OF ILLINOIS AT URBANA-CHAMPAIGN